Wave-CISK in the Tropics

RICHARD S. LINDZEN[1]

Center for Earth and Planetary Physics, Harvard University, Cambridge, Mass. 02138

(Manuscript received 7 June 1973, in revised form 10 September 1973)

ABSTRACT

CISK (Conditional Instability of the Second Kind) is examined for internal waves where low-level convergence is due to the inviscid wave fields rather than to Ekman pumping.

It is found that CISK-induced waves must give rise to mean cumulus activity (since there are no negative clouds), and it is suggested that this mean activity plays an important role in the finite-amplitude equilibration of the system. The most unstable CISK waves will be associated with very short vertical wavelengths [O(3 km)] in order to maximize (in some crude sense) subcloud convergence. Thus, the vertical scale is largely determined by the height of cloud base. The vertical scale, in turn, determines the dispersive relations between horizontal and temporal scales. It is found that there exists a wave-CISK mode which is independent of longitude, and hence independent of the mean zonal flow. Because of this independence, the period of this oscillation should form a prominent line in tropical spectra. This period turns out to be about 4.8 days which is indeed a prominent feature of tropical spectra. It is shown, due to longitudinal inhomogeneities in the tropics (such as land-sea), that the above oscillation must be accompanied by traveling disturbances whose period with respect to the ground will also be 4.8 days and whose longitudinal scales will typically be from 1000–3000 km depending on the mean zonal flow. It is further shown that the existence of the above oscillatory *system* has two additional implications:

(i) The above system is, itself, unstable with respect to gravity waves with horizontal scales on the order of 100–200 km. Such waves may be associated with cloud clusters.

(ii) The above system leads to maximum low-level convergence (and hence, a tendency toward mean cumulus activity) in regions centered about ±6°–7° latitude, thus providing a possible explanation for the position of the ITCZ.

1. Introduction

Since the late 1950's (Riehl and Malkus, 1958) it has been recognized that much of tropical meteorology involves the collective interaction of large-scale meteorological circulations and cumulus convection. The likely mechanism for this interaction was first described by Charney and Eliassen (1964) and given the name "conditional instability of the second kind" (i.e., CISK). Briefly, if the atmosphere is conditionally unstable but unsaturated, and if the surface air is sufficiently warm and moist, then there will exist some height z_c such that if surface air is lifted to that height, it will become convectively unstable, giving rise, presumably, to cumulonimbus hot towers which will rise to some great height (near the tropopause) at which height the surface air is no longer convectively unstable. [See Holton (1972a), Ooyama (1971) and Charney (1971b) for more precise discussions]. In CISK, a low-level convergence field associated with a large-scale meteorological system lifts surface air to z_c, where cumulonimbus convection sets in. The latent heat released in the cumulus convection, in turn, forces the large-scale motion whose low-level convergence gave rise to the convection. Quite obviously, to investigate such an interaction one must somehow be able to parameterize the relation between cumulus "heating" and low-level convergence. While this is the subject of much current research (Ooyama, 1971; Arakawa and Schubert, 1974; Yanai *et al.*, 1973), rather crude, simple procedures are available (Charney, 1971; Yamasaki, 1968; Kuo, 1965). It is not the purpose of this paper to probe deeply into the problem of parameterization; however, of necessity, I will discuss the matter, and in Section 2b present a particular parameterization. Underlying all CISK models is the assumption that deep cumulus convection will not, by itself, maintain the low-level convergence necessary for the maintenance of the clouds. Thus, large-scale, low-level convergence is necessary.

Probably the most widely known applications of CISK involve large-scale systems which, in the absence of viscosity, do not involve low-level convergence: hurricanes (Charney and Eliassen, 1964), the inter-tropical convergence zone (ITCZ) (Charney, 1971a) and barotropic waves (Yamasaki, 1971a). The low-level convergence in these calculations is produced by surface

[1] Alfred P. Sloan Foundation Fellow.

Ekman layers. While this is a plausible possibility for hurricanes (which occur at substantial distance from the equator), the effectiveness of Ekman pumping close to the equator seems dubious. Again we are touching on a matter of significant current investigation (Kuo, 1973). Some recent studies (Holton *et al.*, 1971; Yamasaki, 1971) suggest singular boundary layer pumping for oscillatory systems at critical latitudes (where the Doppler-shifted oscillatory frequency equals the Coriolis parameter); however, this finding has been disputed (Hayashi, 1971) and, in general, there are grounds for doubting this effect (namely, for diurnal oscillations such as sea breezes and tides there is no evidence, at present, for singular boundary layer behavior at 30° latitude which is the critical latitude for diurnal phenomena). Moreover, there exist important motion systems, namely, internal waves (gravity, Kelvin, mixed gravity-Rossby and Rossby) which are highly convergent, and for which there is no need for Ekman pumping in order to produce CISK. I shall refer to this as wave-CISK. This matter has already been investigated by Hayashi (1970) and Yamasaki (1969). In this paper I shall redo these calculations using a different formalism (as well as a somewhat different cumulus parameterization) which I hope will make the physical and mathematical nature of wave-CISK clearer. Although my results are similar to those obtained earlier, there are significant quantitative differences. It may seem strange to readers familiar with earlier work on wave-CISK that one should return to it in view of its failure to account for observed tropical wave systems. These earlier calculations showed that the most unstable waves were gravity waves whose growth rates increased indefinitely with increasing zonal and meridional wavenumbers. Significant instabilities corresponding to observed easterly waves in the tropical troposphere and to observed Kelvin and mixed gravity-Rossby waves in the tropical stratosphere were absent. It is the main purpose of this paper to show that, properly interpreted, the results of wave-CISK are not at all in conflict with the observed behavior of the tropical atmosphere, and can, in fact, explain such disparate phenomena as the existence of cloud clusters, the position of the ITCZ, the prominence of a 5-day period in tropical records, tropospheric easterly waves, stratospheric mixed gravity-Rossby waves, and, possibly, even the formation of hurricanes. Certainly, much of what follows will be speculative but hopefully it may provide a framework for undertaking more comprehensive investigations.

As already mentioned, the present work neglects viscosity. As I shall show in Section 3 this omission may be important, but it should be stressed that internal wave convergence, as described here, is, even in the absence of viscosity, an extremely efficient producer of low-level convergence. Indeed, preliminary calculations which will be described separately suggest that for the systems under consideration here, viscosity reduces low-level convergence.

2. Simple Boussinesq model for gravity wave CISK

In this Section I shall consider two-dimensional linear waves in a stratified, non-rotating, Boussinesq fluid. Clearly, such a system is an unrealistic model for the tropics, but we study it first since it represents the simplest situation for which we can obtain a useful description of wave-CISK. Moreover, as I shall show in subsequent sections, results for rotating, spherical, non-Boussinesq atmospheres (even with relatively complicated basic states) may be interpreted in terms of the results of this simple case.

Our assumed basic state consists of an exponentially stratified, hydrostatic density field; no basic horizontal flow is assumed. Additionally, I restrict myself to hydrostatic perturbations. This is essentially valid for waves whose periods are long compared to the Brunt-Väisälä period [O(5 min)]; since we are considering waves destabilized by cumulus convection whose time scale is O(1 hr), hydrostaticity should be generally valid. Our equations for perturbation fields are

$$\frac{\partial u}{\partial t} = -\frac{1}{\rho_0}\frac{\partial p}{\partial x}, \tag{1}$$

$$\frac{\partial p}{\partial z} = -\rho g, \tag{2}$$

$$\frac{\partial \rho}{\partial t} + w\frac{d\rho_0}{dz} = -Q, \tag{3}$$

$$\frac{\partial u}{\partial x} + \frac{\partial w}{\partial z} = 0, \tag{4}$$

where:

- u perturbation horizontal velocity
- w perturbation vertical velocity
- ρ density perturbation
- g gravitational acceleration
- t time
- x horizontal coordinate
- z vertical coordinate.

We also have

$$\rho = \rho_0(0)e^{-z/H} \quad (H \approx 7.5 \text{ km}), \tag{5}$$

where ρ_0 is a basic density distribution and Q is a thermal forcing (or its analog for a Boussinesq system) due to latent heat release which will eventually be described in terms of the wave fields themselves. For the moment I assume Q *is non-zero within a height range* $z_c < z < z_t$, wherein cumulus hot towers are assumed to exist. I also assume that the x,t dependence is such as to permit the Fourier decomposition of Q into terms

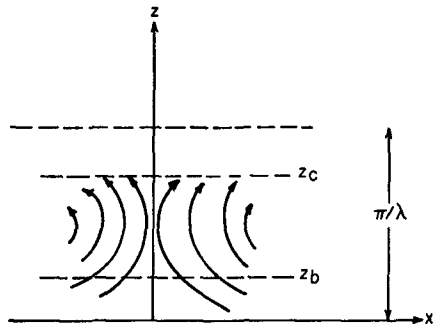

FIG. 1. Schematic illustration of the convergent wave flow field below a cumulus cloud base. The relative positions of the top of the mixed layer, z_b, the height at which surface air becomes convectively unstable, z_c, and π/λ (half the vertical wavelength of the waves) are shown.

which behave as

$$Q=\hat{Q}(z)e^{ik(x-ct)}. \tag{6}$$

Similar forms are assumed for the various perturbation fields so that Eqs. (1)–(4) become

$$-ikc\hat{u}=-\frac{1}{\rho_0}ik\hat{p}, \tag{7}$$

$$\frac{d\hat{p}}{dz}=-\hat{\rho}g, \tag{8}$$

$$-ikc\hat{\rho}-\frac{\hat{w}}{H}\rho_0=-\hat{Q}, \tag{9}$$

$$ik\hat{u}+\frac{d\hat{w}}{dz}=0. \tag{10}$$

One may now reduce Eqs. (7)–(10) to a particularly simple equation for the quantity

$$\tilde{w}=\rho_0^{\frac{1}{2}}\hat{w}, \tag{11}$$

namely

$$\frac{d^2\tilde{w}}{dz^2}+\lambda^2\tilde{w}=\frac{g}{c^2}\hat{Q}\rho_0^{-\frac{1}{2}}, \tag{12}$$

where

$$\lambda^2=\frac{g}{Hc^2}-\frac{1}{4H^2}. \tag{13}$$

My next step is to seek a formal solution to (12) as a functional of Q. The boundary conditions are

$$\tilde{w}=0 \quad \text{at} \quad z=0, \tag{14a}$$

$$\tilde{w}\propto e^{-i\lambda z} \quad \text{for} \quad z>z_t. \tag{14b}$$

If λ is real (14b) is simply the radiation condition. The interpretation of (14b) when λ is complex will be discussed later. My procedure is to obtain the Green's function for the left-hand side of (12) subject to (14a) and (14b) and use it to solve the inhomogeneous problem. The details are in the Appendix. The solution is

$$\tilde{w}=-\frac{\sin\lambda z}{\lambda}\int_{z_c}^{z_t} fe^{-i\lambda z'}dz', \quad 0\leqslant z\leqslant z_c, \tag{15a}$$

$$\tilde{w}=-\frac{\sin\lambda z}{\lambda}\int_{z}^{z_t} fe^{-i\lambda z'}dz'-\frac{e^{-i\lambda z}}{\lambda}\int_{z_c}^{z} f\sin\lambda z'dz', \quad z_c\leqslant z\leqslant z_t, \tag{15b}$$

$$\tilde{w}=-\frac{e^{-i\lambda z}}{\lambda}\int_{z_c}^{z_t} f\sin\lambda z'dz', \quad z\geqslant z_t, \tag{15c}$$

where

$$f\equiv\frac{g}{c^2}Q\rho_0^{-\frac{1}{2}}.$$

The remainder of the solution requires that we know Q. However, before going into detail on this matter, there are some rather general—but essential—statements which can be made.

a. Some general remarks on cumulus heating

If we consider that Q is due to cumulus convection, and that cumulus convection (involving hot towers at least) occurs when air from below some $z=z_b$ (the warm, moist, mixed surface layer) is raised to some height $z=z_c$ (where the surface air becomes unstably buoyant), then if the mechanism bringing air from below z_b to z_c is the mass convergence associated with an internal gravity wave, π/λ [or, if λ is complex, $\pi/\mathrm{Re}(\lambda)$] must be greater than z_c. Otherwise, the air from below z_b will be carried down again before reaching z_c. The situation is schematically illustrated in Fig. 1. Even if π/λ is a little greater than z_c, we may expect the production of cloud air to be diminished. Quantitatively, we might expect diminution to occur when λ [or $\mathrm{Re}(\lambda)$] is larger than that λ for which

$$\pi-\lambda z_c=\lambda z_b,$$

i.e., when

$$\lambda>\pi/(z_c+z_b).$$

In summary wave-CISK will be effective if

$$\lambda\lesssim\pi/(z_c+z_b),$$

relatively less effective when $\pi/(z_c+z_b)<\lambda<\pi/z_c$, and impossible when $\lambda>\pi/z_c$.

Along the above lines, it also appears that the rate of heating due to hot towers must be proportional to the upward mass flux of air from $z\lesssim z_b$ at $z=z_c$. Thus, for example, the definite integral in (15a) must be proportional to $w(z_b)$. If we now use (15a) to evaluate $w(z_b)$, then the coefficient of $w(z_b)$ on the right-hand side of (15a) must equal $\rho_0^{\frac{1}{2}}(z_b)$ [cf. Eq. (11)] in order for the overall scheme to be self-consistent; i.e., for the heating produced by the wave convergence to produce the wave

which produces the convergence. In general, this will be possible only for certain values of λ which may be complex. Such results are necessarily analogous to the findings of Yamasaki (1969) and Hayashi (1970).

Note that the above discussion is consistent with virtually all current methods of cumulus modelling. However, in order to get explicit quantitative results, a specific parameterization for cumulus heating must be chosen. As I have already noted, a variety of models are described in the existing literature. My approach, as described in the next subsection, is crudely consonant with the recent work of Ooyama (1971) and Arakawa (1971). However, as the above discussion shows, the final results ought not be seriously model-dependent in their qualitative (and, as it turns out, even in certain important quantitative) aspects.

b. Cumulus parameterization

I shall, for purposes of this paper, adopt an obviously oversimplified cumulus parameterization. I will consider hot towers rising from $z=z_c$ with a mass flux M_c within the towers equal to $\alpha\rho_0(z_b)w(z_b)$, and constant from z_c to z_t, i.e.,

$$M_c=\alpha\rho_0(z_b)w(z_b)=\text{constant}, \quad z_c\leqslant z\leqslant z_t. \tag{16}$$

The parameter α is taken to be a constant (generally greater than 1); introducing α in (16) is a crude way of indicating that not only is unstable air from below z_b involved in M_c, but also entrained air from above z_b which is lifted above its condensation level. Recall that z_b is the height of the mixed layer, while z_c is the height above which air from below z_b becomes convectively unstable. Note that the lifting condensation level for air below z_b may be less than z_c though no account of this appears to have been taken in any parameterization.

The temperature within the clouds is assumed to lie on a saturated adiabat so that no adiabatic cooling of the updrafts is realized. The heating is, *formally*, taken to arise from the downdrafts in the dry regions between the clouds which compensate the updrafts within the clouds. Given a positive $w(z_b)$, w in the compensating downdraft will be

$$w_{dd}=-\alpha w(z_b)\frac{\rho_0(z_b)}{\rho_0(z)}, \tag{17}$$

and Q will be given by

$$Q=+w_{dd}\frac{d\rho_0}{dz}=\alpha\frac{w(z_b)\rho_0(z_b)}{H}. \tag{18}$$

(N.B. Q, here, is not formally a heating; it is the counterpart of heating for the present Boussinesq fluid).

Eq. (17) appears to suggest that there is no net mass flux due to cumulus convection. However, the actual vertical flow outside clouds is due to the sum of w_{dd} and the large-scale w forced by the cumulus heating. The latter may compensate w_{dd} leading to a net cloud mass transport.

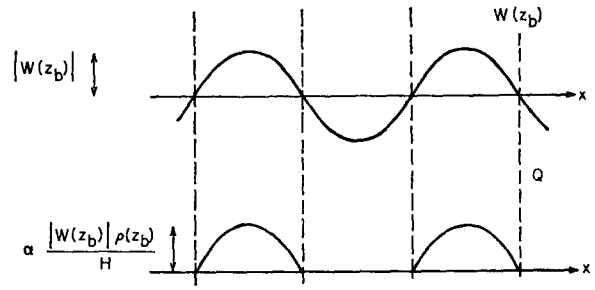

FIG. 2. The cumulus heating Q associated with an oscillatory vertical velocity at z_b, $w(z_b)$.

Now, (18) applies only if $w(z_b)>0$; if $w(z_b)<0$, there is no cumulus activity. Thus, if $w(z_b)$ is monochromatically oscillatory, then at any time t, $w(z_b,x)$ and $Q(x)$ will look as shown in Fig. 2.[2] If Q, as shown in Fig. 2, is to force an oscillation, only its Fourier component at the oscillation's wavenumber can be included in the forcing. Letting

$$w(z_b,x)=|w(z_b)|\cos kx, \tag{19}$$

we then obtain for Q

$$\left.\begin{aligned} &Q=\alpha\frac{w(z_b)\rho_0(z_b)}{H}, \quad -\frac{\pi}{2}<kx<\frac{\pi}{2}\\ &Q=0, \quad \begin{cases} -\pi\leqslant kx\leqslant -\dfrac{\pi}{2}\\ \dfrac{\pi}{2}\leqslant kx\leqslant\pi \end{cases}\\ &Q(kx+2\pi)=Q(kx) \end{aligned}\right\}. \tag{20}$$

If we let

$$Q_0\equiv\alpha\frac{|w(z_b)|\rho_0(z_b)}{H},$$

then

$$Q=\frac{Q_0}{\pi}+\tfrac{1}{2}Q_0\cos kx+\cdots. \tag{21}$$

Note that the cumulus heating induced by a wave of wavenumber k will consist in an average component (indicative of the impossibility of "negative" hot towers), a component with wavenumber k in phase with $w(z_b)$, and higher wavenumbers corresponding to harmonic distortion. Only the second term in (21) enters the original wave equation. However, the fact that wave-CISK inevitably leads to mean heating will play a significant role in my discussion of the finite-amplitude evolution of wave-CISK instabilities. In this

[2] One could equivalently consider $w(z_b, t)$ and $Q(t)$ at a fixed x; this will later prove essential when we have occasion to consider oscillations for which $k=0$.

connection, it should be noted that if the mean term in (21) forces a meridional circulation with significant mean $w(z_b)$, then the coefficient of $\cos kx$ in (21) can rise to a maximum of Q_0, while at the same time the mean term in (21) can decrease to a minimum of zero. For reasons which I will discuss later, I feel that this is unlikely to be an important effect. However, as we shall see, a very similar and important effect can arise when several oscillations with very different space and time scales exist simultaneously.

Before continuing, a few words on the shortcomings of the above parameterization are in order. Using this parameterization of heating, we are, by ignoring cloud entrainment except as it may be parameterized by α, and, associated with this, the presence of cumulus clouds other than "hot towers," distorting the height distributions of cumulus heating and possibly its magnitude as well. We are also ignoring a cooling term due to the re-evaporation of detrained liquid water—a term which Yanai *et al.* (1973) find to be significant. Finally, our parameterization ignores the moisture budget of the atmosphere. As we shall see this will prevent a quantitative evaluation of finite-amplitude evolution. Also, no account is taken of momentum transport by cumulus clouds, though this matter is discussed further in Section 8.

c. *Equations for possible* λ's.

From the above subsection we obtain the following expression for $\hat{Q}$ to be used in Eq. (12):

$$\hat{Q}=\frac{\alpha}{2}\frac{\hat{w}(z_b)\rho_0(z_b)}{H}, \tag{22}$$

$$f=\frac{g}{c^2}\frac{\alpha}{2}\frac{\hat{w}(z_b)\rho_0(z_b)}{H}\rho_0^{-\frac{1}{2}}(0)e^{z/(2H)}$$

$$=\mu\rho_0^{-\frac{1}{2}}(0)\rho_0(z_b)\hat{w}(z_b)e^{z/(2H)}, \tag{23}$$

where $\mu=(\alpha/2)(g/c^2)(1/H)$. Using (23), the integrals in Eqs. (15a), (15b) and (15c) can be explicitly evaluated yielding

$$\rho_0^{\frac{1}{2}}(z)\hat{w}(z)$$

$$=-\frac{\sin\lambda z}{\lambda}\mu\rho_0^{-\frac{1}{2}}(0)\rho_0(z_b)\frac{\hat{w}(z_b)}{[(1/2H)-i\lambda]}$$

$$\times\exp\{z'[(1/2H)-i\lambda]\}\Big|_{z_c}^{z_t}, \quad \text{for} \quad 0\leqslant z\leqslant z_c, \tag{24}$$

$$\rho_0^{\frac{1}{2}}(z)\hat{w}(z)$$

$$=-\frac{\sin\lambda z}{\lambda}\mu\rho_0^{-\frac{1}{2}}(0)\rho_0(z_b)\frac{\hat{w}(z_b)}{[(1/2H)-i\lambda]}$$

$$\times\exp\{z'[(1/2H)-i\lambda]\}\Big|_{z}^{z_t}$$

$$-\frac{e^{-i\lambda z}}{\lambda}\mu\rho_0^{-\frac{1}{2}}(0)\rho_0(z_b)\frac{\hat{w}(z_b)}{[(1/4H^2)+\lambda^2]}$$

$$\times e^{z'/(2H)}\left[\frac{1}{2H}\sin\lambda z'-\lambda\cos\lambda z'\right]\Big|_{z_c}^{z},$$

$$\text{for} \quad z_c\leqslant z\leqslant z_t, \tag{25}$$

$$\rho_0^{\frac{1}{2}}(z)\hat{w}(z)$$

$$=-\frac{e^{-i\lambda z}}{\lambda}\mu\rho_0^{-\frac{1}{2}}(0)\rho_0(z_b)\frac{\hat{w}(z_b)}{[(1/4H^2)+\lambda^2]}$$

$$\times e^{z'/(2H)}\left[\frac{1}{2H}\sin\lambda z'-\lambda\cos\lambda z'\right]\Big|_{z_c}^{z_t},$$

$$\text{for} \quad z\geqslant z_t. \tag{26}$$

As already noted, the actual oscillatory vertical flows outside the clouds will be determined by both $\hat{w}$ and the oscillatory component of the compensating downdrafts. The mean component of the compensating downdrafts will be partially cancelled by the mean w induced by the mean heating; part of the mean heating, however, will be balanced by radiative cooling.

The consistency condition for the above system is obtained by evaluating Eq. (24) at $z=z_b$ to obtain

$$\hat{w}(z_b)=-\frac{\sin\lambda z_b}{\lambda}u\left[\frac{\rho_0(z_b)}{\rho_0(0)}\right]^{\frac{1}{2}}\frac{\hat{w}(z_b)}{[(1/2H)-i\lambda]}$$

$$\times\exp\{z'[(1/2H)-i\lambda]\}\Big|_{z_0}^{z_t}, \tag{27}$$

or since

$$\mu=\frac{\alpha}{2}\frac{g}{c^2H}=\frac{\alpha}{2}\left(\lambda^2+\frac{1}{4H^2}\right),$$

$$\frac{\alpha}{2}\left(\frac{1}{2H}+i\lambda\right)\frac{\sin\lambda z_b}{\lambda}\left[\frac{\rho_0(z_b)}{\rho_0(0)}\right]^{\frac{1}{2}}$$

$$\times\exp\{z'[(1/2H)-i\lambda]\}\Big|_{z_0}^{z_t}=-1. \tag{28}$$

Now, in general, $|\lambda z_b|\ll 1$, so that $\lambda^{-1}\sin\lambda z_b\approx z_b$. Also $[\rho_0(z_b)/\rho_0(0)]^{\frac{1}{2}}\approx 1$. Finally, $z_c/2H\ll 1$, so that $e^{z_c/2H}\approx 1$. Eq. (28) then becomes

$$\frac{\alpha z_b}{2}\left(\frac{1}{2H}+i\lambda\right)(\exp\{z_t[(1/2H)-i\lambda_r+\lambda_i]\}$$

$$-\exp[z_c(-i\lambda_r+\lambda_i)])\approx -1, \tag{29}$$

where λ has been rewritten

$$\lambda=\lambda_r+i\lambda_i.$$

Taking the real and imaginary parts of (29), one gets

$$\left(\frac{1}{2H}-\lambda_i\right)(\exp\{z_t[(1/2H)+\lambda_i]\}\cos\lambda_r z_t-e^{z_c\lambda_i}\cos\lambda_r z_c)$$
$$+\lambda_r(\exp\{z_t[(1/2H)+\lambda_i]\}\sin\lambda_r z_t-e^{z_c\lambda_i}\sin\lambda_r z_c)$$
$$\approx-\frac{2}{\alpha z_b}, \quad (30)$$

and

$$\lambda_r(\exp\{z_t[(1/2H]+\lambda_i]\}\cos\lambda_r z_t-e^{z_c\lambda_i}\cos\lambda_r z_c)$$
$$-\left(\frac{1}{2H}-\lambda_i\right)(\exp\{z_t[(1/2H)+\lambda_i]\}\sin\lambda_r z_t$$
$$-e^{z_c\lambda_i}\sin\lambda_r z_c)\approx 0. \quad (31)$$

Substituting (31) into (30) and multiplying the result by z_t, one gets

$$\left\{\frac{[(z_t/2H)-\lambda_i z_t]^2}{\lambda_r z_t}+\lambda_r z_t\right\}(\exp\{z_t[(1/2H)+\lambda_i]\}\sin\lambda_r z_t$$
$$-e^{z_c\lambda_i}\sin\lambda_r z_c)\approx-\frac{2z_t}{\alpha z_b}. \quad (32)$$

For ease of calculation we now introduce the labels

$$X=\frac{z_t}{2H}, \quad Y=\lambda_r z_t, \quad U=\lambda_i z_t, \quad \gamma=\frac{z_c}{z_t} \quad \beta=\frac{4H}{\alpha z_b}.$$

Eqs. (32) and (31) then become

$$\left[\frac{(X-U)^2}{Y}+Y\right][e^X e^U\sin Y-e^{\gamma U}\sin\gamma Y]=-\beta X, \quad (32a)$$

$$Y[e^X e^U\cos Y-e^{\gamma U}\cos\gamma Y]$$
$$-(X-U)[e^X e^U\sin Y-e^{\gamma U}\sin\gamma Y]=0. \quad (31a)$$

We will see *a posteriori* that X/Y, $U/Y\ll 1$, and, in addition, that $\gamma\ll 1$. Making use of this, (32a) and (31a) may be approximated by

$$Y[e^{(X+U)}\sin Y-\sin\gamma Y]\approx-\beta X, \quad (32b)$$

$$e^{(X+U)}\cos Y\approx\cos\gamma Y, \quad (31b)$$

which finally may be rewritten

$$Y\tan Y\approx-\frac{\beta X+Y\sin\gamma Y}{\cos\gamma Y}, \quad (33)$$

$$U=-X-\ln\left(\frac{\cos Y}{\cos\gamma Y}\right). \quad (34)$$

We may now solve (33) for Y from which λ_r may be deduced. Only those solutions for which $\cos Y/\cos\gamma Y>0$ are proper, and for these (34) may be solved for U from which λ_i may be deduced.[3]

Before proceding to the solution of (33) and (34), it will be useful to show how our solution for λ determines the stability of a given solution.

d. λ's and stability

I have considered solutions of the form

$$e^{ik(x-ct)-i\lambda z} \quad (35)$$

above $z=z_t$. Now from (13) we have

$$\lambda^2=\frac{g}{Hc^2}-\frac{1}{4H^2},$$

or, upon solving for c,

$$\frac{Hc^2}{g}=\frac{1}{\lambda^2+(1/4H^2)}. \quad (36)$$

It is clear from (35) that complex λ implies complex c, and from (35) that complex c implies exponential time growth or decay of the wave. As we have seen in Section 2c, our consistency equation does not completely determine λ. What it does do, is determine λ_i and $|\lambda_r|$; it does not determine the sign of λ_r. In order to determine the sign of λ_r, another condition must be imposed, and the radiation condition is the only possibility which suggests itself. For internal gravity waves (and Rossby waves for that matter), positive λ_r corresponds to downward phase propagation and upward energy flux, while negative λ_r corresponds to upward phase propagation but downward energy flux. Since our only energy source is below $z=z_t$, the choice of positive λ_r is indicated. Implicit in the above, moreover, has been the choice of a positive real part for c. With this in mind, it is easily shown from (36) that if the imaginary part of λ (λ_i) is negative, then the imaginary part of c (c_i) will be positive, while if λ_i is positive, then c_i will be negative. Reference to Eq. (35) shows that positive c_i implies instability while negative c_i implies stability. In addition, we see that for $z>z_t$, unstable waves decay with height, while stable wave perturbations grow with height. This is heuristically reasonable. Consider a neutral wave existing at some time $t=0$ at which time the wave becomes unstable. Since the source of instability is below $z=z_c$, we expect growth to manifest itself initially at lower levels giving rise to the appearance of decay with height. Similarly, should the neutral wave become stable, the decay will manifest itself earlier at lower levels giving rise to the appearance of growth with height. Although our discussion is still dealing only with simple internal gravity waves, the above

[3] Note that if Y is a solution, so is $-Y$.

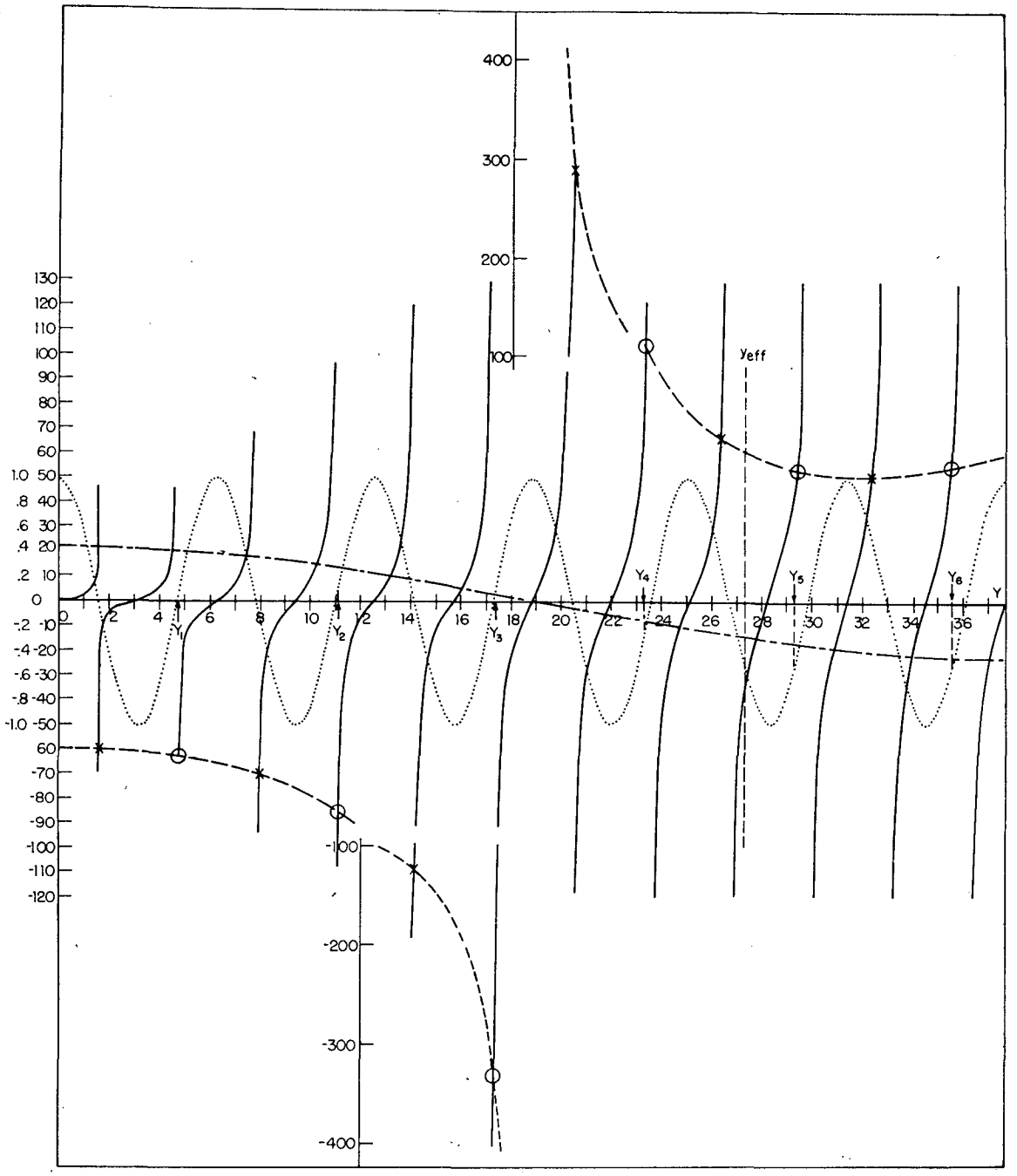

FIG. 3. Associated with the large scale at the left of the figure (and present in expanded form near the middle of the figure) are the functions $Y \tan Y$ (solid line) and $(-\beta X + Y \sin \gamma Y)/\cos \gamma Y$ (dashed line). When the intersection of these curves occurs at a value of Y for which $(\cos Y/\cos \gamma Y) > 0$, that value of is an eigensolution, and is marked by an open circle. The small scale of the left is associated with the functions $\cos Y$ (dotted lines) and $e^{-X} \cos \gamma Y$. When for an eigensolution $|\cos Y| > |e^{-X} \cos \gamma Y|$, then that eigensolution is unstable. Details are given in the text. For this figure $\gamma = 1/12$, $X = 0.8$ and $\beta X = 60$.

considerations are also relevant to more general waves on a rotating sphere (or equatorial β-plane).

A few more points must be discussed before proceeding. From Section 2c we see that given z_c, z_t and αz_b, λ may be determined, and given λ we see from (36) that c is determined (in this case c is independent of k, though this will not remain the case on a sphere or an equatorial β-plane). From (35) we see that for the present situation, the growth rate kc_i will, in fact, grow linearly with k. While there is some real meaning to this

TABLE 1. Solution for Y and U for various choices of z_c, z_t, and β (see text for details).

z_t (km)	12	12	12	15	15	15
z_c (km)	1	1	1.2	1	1	1.2
X	0.8	0.8	0.8	1.0	1.0	1.0
βX	60	30	60	60	30	60
γ	1/12	1/12	1/10	1/15	1/15	0.08
Y_1/π	1.52	1.55	1.52	1.52	1.55	1.52
U_1	1.70	.964	1.69	1.50	.777	1.50
Y_2/π	3.54	3.60	3.53	3.55	3.61	3.54
U_2	0.733	−0.139	0.712	0.560	−0.264	0.538
Y_3/π	5.52	5.55	5.48	5.55	5.65	5.52
U_3	0.106	−1.11	0.116	−0.062	−1.16	−0.091
Y_4/π	7.43	7.27	7.39	no solution		7.44
U_4	−0.281	−1.51	−0.119			−0.507
Y_5/π	9.34	9.15	9.34	9.39	9.10	9.35
U_5	−0.330	−0.999	−0.066	−0.838	−2.06	−0.591
Y_6/π	11.32	11.18		11.30	11.06	11.31
U_6	−0.211	−0.644		−0.800	−1.37	−0.475
Y_7/π				13.27	13.11	
U_7				−0.640	−1.01	

result, there must be a limit to how large k can get. Clearly, if the time scale for the wave, $(kc_r)^{-1}$, becomes less than some time scale τ which is somewhat in excess of the lifetime of a cumulonimbus hot tower, then wave-CISK will be impossible. As we shall see later this leads naturally and conveniently to an estimate of the scale of "cloud clusters" (Martin and Suomi, 1972). Finally, I would like to note that while under conditions of instability, growth rates increase with increasing k, the condition for neutral stability is the same for all k's (i.e., independent of k). This is rather different from other stability problems [such as Bénard convection (Chandrasekhar, 1961) or baroclinic instability in two-level models (Phillips, 1954)] where, as the parameter leading to instability is increased, the first mode to become unstable is the mode which is most unstable slightly above the stability limit. In these earlier problems a preferred scale was easily identified—even on the neutral curve. Scale selection in the present problem will no longer be such a straightforward matter.

e. Explicit evaluation of λ

In solving (33) I merely search for all roots subject to the constraints

$$\gamma Y < \pi, \tag{37}$$

$$\frac{\cos Y}{\cos \gamma Y} > 0. \tag{38}$$

Although there is the implicit recognition that if z_b can be specified, then solutions for which

$$\frac{\pi z_c}{(z_c+z_b)} < \gamma Y < \pi \tag{39}$$

are going to be inefficient for CISK (*viz.* Section 2a), no explicit account of this will be taken initially. We will, however, have to introduce this consideration in those situations where the most unstable seeming solution occurs for γY in the range given by (39), while other solutions (almost as unstable) exist for

$$\gamma Y \lesssim \frac{\pi z_c}{z_c+z_b}. \tag{40}$$

The nature of solutions to (33) is shown in Fig. 3 where the right- and left-hand sides of (33) are plotted as functions of Y. The intersections of the two curves yield solutions to (33). Also plotted are $\cos Y$ and $e^{-X}\cos\gamma Y$. The solutions to (33) which satisfy (38) are marked by open circles; those which do not are marked by crosses. I have chosen $\gamma = \frac{1}{12}$, $\beta X = 60$ and $X = 0.8$. We see that there should typically be about $1/(2\gamma)$ possible solutions for Y [$1/(2\gamma) = 6$ for the case shown]; these solutions will be designated as Y_n. If for a given Y_n, $|\cos Y_n| > e^{-X}|\cos\gamma Y_n|$, then from (34) we see that the associated U_n will be negative and the resulting waves will be unstable. As may be seen from Fig. 3, this situation may be brought about by 1) increasing X (or equivalently, z_t), and 2) for a given X, decreasing β (or, equivalently, increasing αz_b). Similarly, there is a tendency for Y_n to approach an integral multiple of π as n increases so that $|\cos Y_n|$ approaches its maximum value of 1. This tends to make the largest Y_n's correspond to the most unstable solutions. Counteracting this effect is the fact that $\cos\gamma Y$ is very small in the neighborhood of $\gamma Y = \pi/2$ which tends to destabilize Y_n's in this neighborhood. By direct calculation, I find that the most unstable Y_n's do, in fact, lie between $Y = \pi/(2\gamma)$ and $Y = \pi/\gamma$. It also turns out to be the case that the smaller γ (or, equivalently, z_c) is, the more unstable is the most unstable solution. The precise numerical results for the case shown in Fig. 3 are given in Table 1; similar results are given for other choices

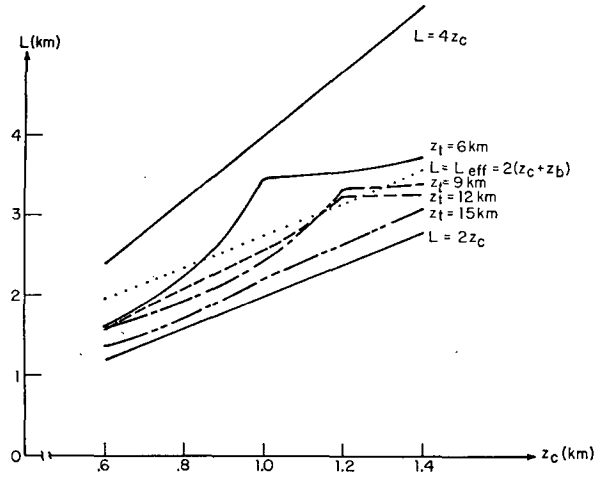

FIG. 4. The vertical wavelength L of the most unstable wave-CISK mode as a function of z_c for several choices of z_t. Also shown are $L=2z_c$ [the shortest wavelength for which wave-CISK is possible], $L=L_{eff}=2(z_c+z_b)$, where z_b has been taken as 0.38 km [the approximate shortest wavelength for which fully efficient wave-CISK may take place], and $L=4z_c$.

of X, γ and β. These results simply serve to confirm the above discussion.

Let us, for the moment, make the speculative leap of assuming that wave-CISK, as described here, is *somehow* related to actual waves observed in the tropical atmosphere (tropospheric easterly waves, mixed gravity-Rossby waves in the stratosphere, etc.). Now, over a substantial part of the lifetime of such waves, they appear to be neither growing nor decaying significantly. Thus we might suppose that the net effect of the *mean* cumulus activity resulting from wave instabilities is to produce a mean state for the atmosphere wherein z_t, z_c, α and z_b are such that the most unstable solution is only marginally unstable (i.e., almost neutral), while the remaining solutions are actually stable. In order to examine this supposition, I show in Fig. 4 the variation of L_N [$=2\pi/\mathrm{Re}(\lambda_N)$; N is the value of n for the most unstable solution] as a function of z_c for various choices of z_t for the marginally unstable solutions described above. In Fig. 5 I show as functions of z_c for various z_t's, the values of αz_b for which the most unstable solutions are, in fact, neutral. In addition I show in Fig. 4 that $L_N=2z_c$ (the smallest L for which wave-CISK is possible) and $L=4z_c$. Note that all our solutions lie between these two curves. If we take for z_b, $z_b\approx 0.38$ km (corresponding to $p=950$ mb), then $L_{\mathrm{eff}}=2z_c+2z_b$ is the wavelength such that shorter wavelengths will have "inefficient" wave-CISK; L_{eff} is also shown in Fig. 4. We see that most of our solutions are in the inefficient region. It turns out that if L_N is in the inefficient region, L_{N-1} is generally very close to L_{eff}. If then, at each z_c for which L_N is substantially within the inefficient region, we ask for what value of αz_b, L_{N-1} will be neutrally stable, we obtain the dotted curves in Fig. 5. Since the dotted curves are rather close to the solid curves, we may conclude that the more efficient solutions will, in fact, be realized.

The above results lead to some conclusions which will prove important in later discussions. First, although I formally identify z_t with the height to which hot towers reach, it is obvious that we could just as well consider it to be a general parameter determining the height distribution of cumulus "heating" [this is what was done by Geisler (1972)]. Under these circumstances, z_t would be parameterizing not only the height of hot towers but also variations in static stability with height, etc. From Fig. 5 we see, not surprisingly, that z_t plays an important role in determining the critical αz_b for the neutrality of the most unstable waves CISK modes. On the other hand, we see from Fig. 4 that L, for these modes, is primarily determined by z_c, and the effect of z_t on L is rather small (especially when account is taken of wave-CISK efficiency). Over most of the tropics z_c is both well defined and rather constant [O (1 km)]. From Fig. 4 we see that this implies that *wave-CISK modes will be characterized by $L\approx 3$ km independently of almost any detailed aspects of our cumulus parameterization.* This fact will play a crucial role in our later discussion. It should be noted that $L\approx 3$ km tends to maximize subcloud convergence for $z_c\approx$O(1 km). It may, therefore, be expected that variations of z_c will lead to proportional changes in L. Additionally, Fig. 5 suggests that a typical critical value for αz_b is about 0.4 km. For $z_b\approx 0.38$ km, this implies that $\alpha\approx 1$. Now, from data analyses by Reed and Recker (1971) and Yanai *et al.* (1973) it appears that $\alpha\approx 4$–6 in actual tropical wave disturbances. This would appear to suggest that the real atmosphere is highly unstable with respect to wave-CISK instability in contradiction to our supposition of neutrality. The uncertainties of both the present cumulus parameter-

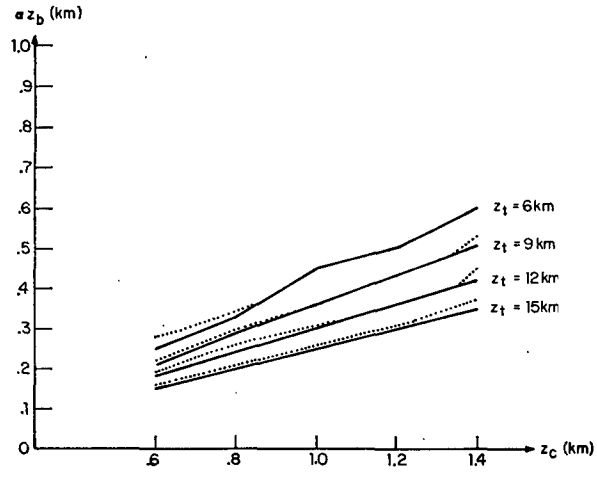

FIG. 5. The value αz_b for which the most unstable wave-CISK mode is neutrally stable as a function of z_c for various choices of z_t. If the most unstable mode is one for which wave-CISK ought to be inefficient, the value of αz_b for the neutrality of the nearest efficient mode is also shown (dotted curves).

ization and the above-mentioned data analyses are probably so great as to make it unwise to make too much of the contradiction. Nevertheless, there are two compelling reasons for believing the preceding calculations strongly underestimate the value of αz_b needed for neutrality. These reasons will only be briefly cited here, although the first will be discussed in greater detail later. First, the above analysis assumes the undisturbed atmosphere is horizontally uniform. Thus, a given amount of low-level convergence will lead to the same amount of cumulus activity—regardless of location. However, it is conceivable that at certain tropical longitudes the surface air may be sufficiently dry (over land, for example) and/or cool so as to leave the air relatively "un-CISKable." Let the fraction of tropical longitudes which are "CISKable" be η; it will be shown in Section 5 that the critical values of αz_b will be raised to η^{-1} times the values indicated in Fig. 5. The physical reason for this is simply that cumulus heating in the CISKable regions must now force the waves in both the CISKable and non-CISKable regions. Second, I have neglected viscosity. However, as will be seen in Section 3, we will be considering waves in a rotating spherical atmosphere for which $L \approx 3$ km as above, but where periods may be several days. For such waves, internal friction will be important—even if low values of eddy viscosity are assumed. Although I shall not deal explicitly with viscous calculations in this paper, it is obvious that internal friction will inhibit the propagation of internal waves from the region of cumulus heating to the mixed surface layer, and hence diminish wave convergence. This effect may be compensated to a certain extent in quasi-geostrophic waves where friction near the surface leads to Ekman boundary layer pumping. Perhaps the most serious reason is that since $w(z_b)$ is oscillatory, if its amplitude is not large enough, there may not be sufficient time for $w(z_b)$ to bring air from z_b to z_c. Consequences of such amplitude-dependent effects will be described in a separate paper.

Although I shall not devote a great deal of time to the vertical structure implied by Eqs. (24)–(26), it may prove of interest to the reader to see the distribution with height of the amplitude and phase of both $\tilde{w}$ and $d\tilde{w}/dz$ [recall $\tilde{w}=\rho_0^{\frac{1}{2}}(z)\hat{w}$] for a typical situation. The former is shown in Fig. 6, the latter in Fig. 7. Both quantities have been divided by $\mu\rho_0^{-\frac{1}{2}}(0)\rho_0(z_b)\hat{w}(z_b)$; and in each case I have taken $L=3.24$ km, $z_c=1.2$ km, and $z_t=12$ km. Also shown in Fig. 6 is the magnitude of the compensating downdraft associated with the wave [divided by $\mu\rho_0^{-\frac{1}{2}}(0)\rho_0(z_b)w(z_b)e^{z/2H}$]; the phase of the compensating downdraft is 180°. In both figures we see that L, not surprisingly, is the characteristic scale of the vertical structure. In Fig. 6, we see that $\hat{w}$ is mostly out of phase with the oscillatory component of the compensating downdraft, w_{dd}, in the region $z_c<z<z_t$. However, every 3.24 km there is a thin region where $\hat{w}$ is in phase with w_{dd}; $\hat{w}$'s amplitude in these regions is small

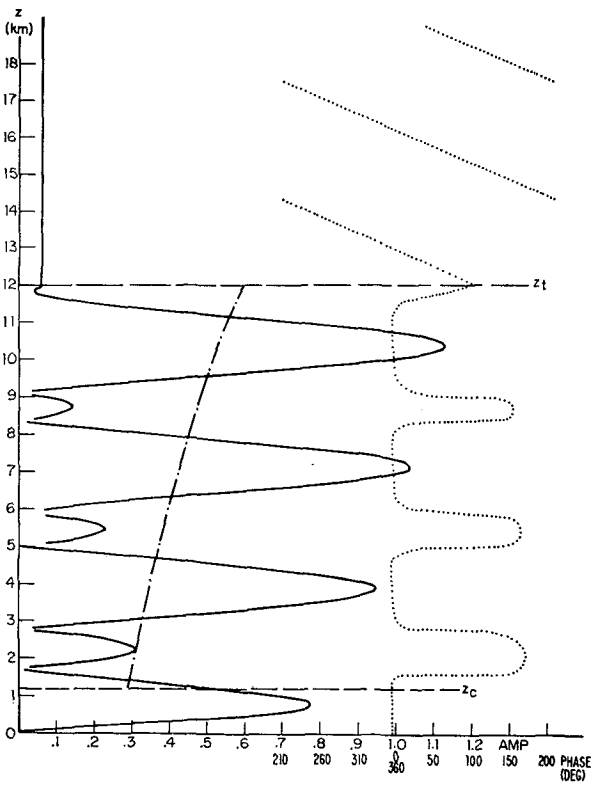

FIG. 6. The amplitude of

$$\hat{w}\ \{\text{multiplied by } [\rho_0^{\frac{1}{2}}(z)/(\mu\rho_0^{-\frac{1}{2}}(0)\rho_0(z_b)\hat{w}(z_b)]\}$$

(solid line) and the oscillatory part of

$$w_{dd}\ [\text{divided by } (\mu\rho_0^{-\frac{1}{2}}(0)\rho_0(z_b)\hat{w}(z_b)e^{z/2H}]$$

(dot-dashed line) as functions of height z. Also shown is the phase of $\hat{w}$ (dotted lines). For the case shown, $z_c=1.2$ km, $z_t=12$ km and $L=3.24$ km.

though. In general, the average of $\hat{w}$ over the region $z_c<z<z_t$ tends to cancel the oscillatory part of w_{dd}. The sum of the oscillatory part of w_{dd} and $\hat{w}$ would, in the region $z_c<z<z_t$, tends to oscillate between $\pm w_{dd}$ with a wavelength L. Above $z=z_t$ the amplitude of a wave-CISK disturbance will be very small, consistent with the general situation when the thickness of the source of thermal excitation is greater than the vertical wavelength of the excited wave (Lindzen, 1966; Green, 1965). The distribution of $d\tilde{w}/dz$ in Fig. 7 is of some interest since in the present model (as well as under more realistic conditions) the horizontal velocity oscillation is approximately proportional to $d\tilde{w}/dz$ [see Eq. (4)]. Fig. 7 implies that the oscillating part of the horizontal velocity will appear as a standing wave between z_t and the ground with seven reversals in sign; this is surprisingly consistent with the observations of Madden and Zipser (1970).

Finally, Figs. 6 and 7 suggest why z_c seems to play a more prominent role in determining the nature of wave-CISK instabilities than does z_t. Namely, due to the short vertical wavelengths of the most unstable waves,

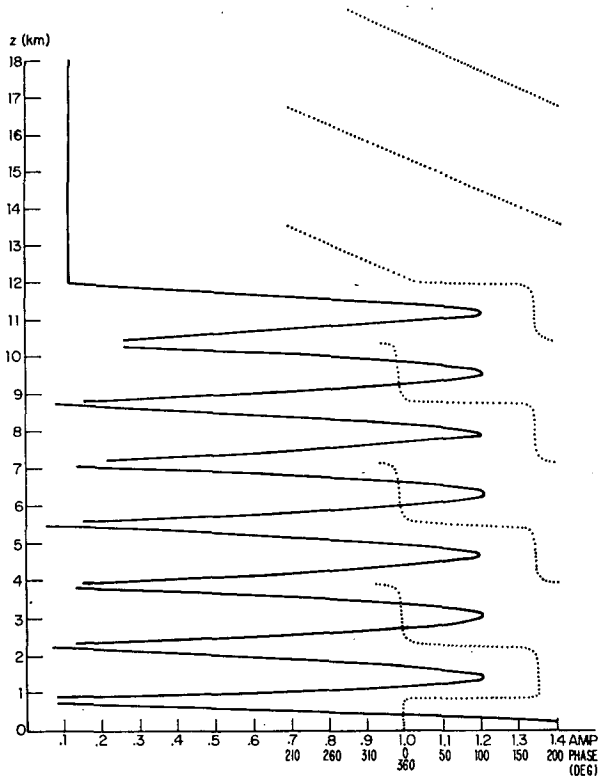

FIG. 7. The amplitude (solid lines) and phase (dotted lines) of $d\tilde{w}/dz$ $[\tilde{w}=\hat{w}\rho_0^{\frac{1}{2}}(z)]$ as a function of height for the same case shown in Fig. 6. The magnitude has again been divided by $\mu\rho_0^{-\frac{1}{2}}(0)\rho_0(z_b)\hat{w}(z_b)$.

that portion of the waves excited in the upper parts of the region $z_c<z<z_t$ is significantly destroyed by interference before reaching the region below z_c. It is the portion of the wave excited in the region just above z_c which is most important in determining $w(z_b)$.

3. Wave-CISK in a rotating spherical atmosphere with a static basic state

The problem of thermally forced waves in a rotating spherical atmosphere with a static basic state (where, however, the basic temperature T_0 may vary with height) is exactly the problem dealt with in the theory of thermal tides in the atmosphere (see Chapman and Lindzen, 1970). In atmospheric tidal theory, one seeks solutions of the form

$$q=q(\theta,z)e^{i(\omega t+s\phi)}, \tag{41}$$

where q is any field, θ latitude (or colatitude), z altitude, t time, ϕ longitude, ω frequency, and s zonal wavenumber. At the equator $k=s/a$ and $c=-\omega/k$. The equations for tidal perturbations are reduced to a single equation for the θ and z dependence of a variable y, where

$$y=-\frac{1}{\gamma p_0}\left(i\omega p+w\frac{dp_0}{dz}\right)\left[\frac{p_0}{p_0(0)}\right]^{\frac{1}{2}}, \tag{42}$$

where $\gamma=c_p/c_v$, p is the perturbation pressure, p_0 the basic pressure, and w the perturbation vertical velocity. For an atmosphere where T_0 is not a constant, y is, in general, the most convenient field to work with. Other fields are readily related to y and its derivatives. Now, the equation for y is separable in its θ and z dependence. The equation for θ dependence is Laplace's tidal equation, which, for each choice of ω and s, has an infinite number of eigensolutions $\{\Theta_n(\theta)\}$ (known as Hough functions), and eigenvalues $\{h_n\}$ (known as equivalent depths). The latter are generalized measures of the horizontal wavenumber associated with each Hough mode (Lindzen, 1971b). Next, the thermal excitation is expanded in terms of the Hough functions

$$J=\left[\sum_n J_n(z)\Theta_n(\theta)\right]e^{i(\omega t+s\varphi)}, \tag{43}$$

where J is the oscillatory forcing in terms of energy per unit mass per unit time. The $J_n(z)$'s then force the vertical structure equation for each mode; i.e., if we write

$$y=\left[\sum_n y_n(z)\Theta_n(\theta)\right]e^{i(\omega t+s\varphi)}, \tag{44}$$

then

$$\frac{1}{H}\frac{d}{dz}\left(H\frac{dy_n}{dz}\right)+\left[\frac{R}{gh_nH}\left(\frac{dT_0}{dz}+\frac{g}{c_p}\right)-\frac{1}{4H^2}\right]y_n =\frac{1}{H^2}\frac{\kappa J_n}{\gamma gh_n}\left[\frac{p_0(z)}{p_0(0)}\right]^{\frac{1}{2}}, \tag{45}$$

where $H=RT_0/g$, R is the gas constant for air $[=c_p-c_v]$, $\kappa=\gamma-1/\gamma$, $\gamma=c_p/c_v$, and c_p and c_v are the constant pressure and constant volume heat capacities for air. Eq. (45) assumes a much simpler form when

$$x=\int_0^z\frac{dz}{H} \tag{46}$$

is introduced in place of z:

$$\frac{d^2y_n}{dx^2}+\left[\frac{1}{h_n}\left(\kappa H+\frac{dH}{dx}\right)-\frac{1}{4}\right]y_n=\frac{\kappa J_n}{\gamma gh_n}e^{-x/2}. \tag{47}$$

It turns out that w can also be expanded in terms of $\{\Theta_n\}$:

$$w=\left[\sum_n w_n(x)\Theta_n(\theta)\right]e^{i(\omega t+s\varphi)}, \tag{48}$$

$$w_n=\gamma h_n e^{x/2}\left[\frac{dy_n}{dx}+\left(\frac{H}{h_n}-\frac{1}{2}\right)y_n\right]. \tag{49}$$

Indeed, an equation similar to, but more complicated than, (47) could be written down for w_n; however, it is generally easier to work with (47) and (49). My procedure for parameterizing J_n is completely analogous

to the procedure used in Section 2b. I now obtain

$$\frac{J_n}{c_p}=w_{ddn}\left(\frac{dT_0}{dz}+\frac{g}{c_p}\right)$$
$$=\frac{\alpha\rho_0(z_b)w_n(z_b)}{2\rho_0(z)}\left(\frac{dT_0}{dz}+\frac{g}{c_p}\right)$$
$$=\frac{\alpha\rho_0(z_b)w_n(z_b)}{2\rho_0(z)H}\frac{g}{R}\left(\frac{dH}{dx}+\kappa H\right), \quad \text{for } z_c\leqslant z\leqslant z_t \quad (50)$$
$$=0, \quad \text{for } z<z_c \text{ and } z>z_t.$$

[N.B. $p_0=\rho_0 gH=p_0(0)e^{-x}$.]

The above system can be investigated in a manner analogous to that used in Section 2; i.e., $h_n^{\frac{1}{2}}$ will now play a role similar to that played by λ in section 2. It turns out that if the imaginary part of $h^{\frac{1}{2}}$ is positive our solution will be unstable. In brief, we solve (47) for $y\ (z,h)$, evaluate (48) at $z=z_b$, and find those h's for which self consistency is possible. We would then find the value of αz_b for which the most unstable solution is neutral. This procedure will, in general, be rather difficult for arbitrary distributions of $T_0(z)$. Some simplification can be obtained if we anticipate that the characteristic vertical scale for our solutions will be much smaller than the scale of variation for $T_0(z)$. Then, a Green's function for (47) can be formed using WKB approximations (Morse and Feshbach, 1953) to the solutions of the homogeneous part of (47); i.e.,

$$\frac{\exp\left(\pm i\int^x \lambda dx\right)}{\sqrt{\lambda}},$$

where

$$\lambda^2=\frac{1}{h}\left(\kappa H+\frac{dH}{dx}\right)-\frac{1}{4},$$

and using

$$\frac{d}{dx}\left[\frac{\exp\left(\pm i\int^x \lambda dx\right)}{\sqrt{\lambda}}\right]\approx\pm i\lambda\left[\frac{\exp\left(\pm i\int^x \lambda dx\right)}{\sqrt{\lambda}}\right]$$

in evaluating (49). For, the purposes of this paper, however, I shall simplify things still further by assuming the idealization of an isothermal basic state. When $T_0=$ constant, it is, in fact, practical to directly consider the equation for $w_n(z)$, or $\tilde{w}_n(z)$ $[=\rho_0^{\frac{1}{2}}w_n(z)$ just as in Section 2]; the equation obtained [using (46), (47) and (49)] is

$$\frac{d^2\tilde{w}_n}{dz^2}+\left(\frac{\kappa}{hH}-\frac{1}{4H^2}\right)\tilde{w}_n=\frac{\kappa}{hH}\frac{\alpha}{2}\rho_0(z_b)w_n(z_b)\rho_0^{-\frac{1}{2}}(0)e^{z/2H},$$
$$\text{for } z_c\leqslant z\leqslant z_t, \quad (51)$$
$$=0, \quad \text{for } z<z_c,\ z>z_t,$$

which is exactly the equation solved in Section 2 except that the quantity $\kappa/(hH)$ replaces $g/(Hc^2)$. Thus, most results obtained in Section 2 can be taken over completely for the case of the rotating spherical atmosphere. In particular, λ^2 in the earlier problem is related to h by

$$\lambda^2=\left(\frac{\kappa}{hH}-\frac{1}{4H^2}\right), \quad (52)$$

which may be solved to obtain the values of $h^{\frac{1}{2}}$ corresponding to the values of λ obtained in Section 2. Once we obtain the value of $h^{\frac{1}{2}}$ corresponding to the most unstable solution (at neutral stability), we must next find those values of ω, s and n for which this value of h is an eigenvalue of Laplace's tidal equation. In general, this, too, is a rather cumbersome problem (see Longuet-Higgins, 1967); however, for tropical waves it will suffice to approximate a rotating spherical atmosphere by an atmosphere on an equatorial β-plane (Lindzen, 1967, 1971a, 1972; Lindzen and Matsuno, 1968; Holton and Lindzen, 1968). On the equatorial β-plane, $n=-1$ corresponds to a westerly Kelvin wave for which

$$\omega_{-1}\approx-\sqrt{gh}\frac{s}{a}, \quad (53)$$

$$\Theta_{-1}\approx e^{-\xi^2/2}, \quad (54)$$

where

$$\xi=y/[gha^2/(4\Omega^2)]^{\frac{1}{4}}, \quad \Omega=2\pi \text{ day}^{-1}, \quad (55)$$

a is the radius of the earth and y the northward distance from the equator. For $n=0$, we have a westerly gravity wave for which

$$\omega_0\approx-\frac{1}{2}\left[\frac{s}{a}\sqrt{gh}+\left(gh\frac{s^2}{a^2}+4\beta\sqrt{gh}\right)^{\frac{1}{2}}\right], \quad (56)$$

where $\beta=2\Omega/a$, and an easterly mixed gravity-Rossby wave for which

$$\omega_0\approx-\frac{1}{2}\left[\left(gh\frac{s^2}{a^2}+4\beta\sqrt{gh}\right)^{\frac{1}{2}}-\frac{s}{a}\sqrt{gh}\right]. \quad (57)$$

In both cases

$$\Theta_0\approx\xi e^{-\xi^2/2}. \quad (58)$$

For $n\geqslant 1$ there are easterly and westerly gravity waves for which

$$\omega_n\approx\pm\left[gh\frac{s^2}{a^2}+(2n+1)\frac{2\Omega}{a}\sqrt{gh}\right]^{\frac{1}{2}}, \quad (59)$$

and an easterly Rossby wave for which

$$\omega_n\approx\frac{\frac{2\Omega}{a}\frac{s}{a}}{\left[\frac{s^2}{a^2}+(2n+1)\frac{2\Omega}{a}\frac{1}{\sqrt{gh}}\right]}. \quad (60)$$

Corresponding to the above ω_n's, we have

$$\Theta_n \approx \frac{[-2nqH_{n-1}(\xi)+H_{n+1}(\xi)]e^{-\xi^2/2}}{\left[q^2+\frac{n+1}{n}\right]^{\frac{1}{2}}}, \tag{61}$$

where

$$q=\frac{1+\frac{s}{a\omega}\sqrt{gh}}{1-\frac{s}{a\omega}\sqrt{gh}}, \tag{62}$$

and $H_n(\xi)$ is an Hermite polynomial of order n. Note that for $n \geq 1$, the distribution of Θ_n depends on both k and wave type and direction (which determines the dependence of ω on k). We will have to consider the implications of this later, in Section 5.

When $h^{\frac{1}{2}}$ is complex then the ω's in (53), (56), (57), (59) and (60) will also be complex, implying, when $\mathrm{Im}(\sqrt{gh})>0$, instability. If we let

$$\sqrt{gh}=(\sqrt{gh})_r+i(\sqrt{gh})_i, \tag{63}$$

and if we assume we are near neutral stability, then

$$\left|\frac{(\sqrt{gh})_i}{(\sqrt{gh})_r}\right| \ll 1. \tag{64}$$

Then, if we write

$$\omega_n=\omega_{n_r}+i\omega_{n_i},$$

$$\omega_{n_i} \approx \left(\frac{d\omega_n}{d\sqrt{gh}}\right)_{\sqrt{gh}_{\text{neutral}}} (\sqrt{gh})_i. \tag{65}$$

Thus, $d\omega_n/d(gh)^{\frac{1}{2}}$, as evaluated for $(gh)^{\frac{1}{2}}$ neutral, is a measure of the growth rate for wave-CISK instabilities. The formal expressions obtained by differentiating (53), (56), (57), (59) and (60) are as follows:

$$\frac{d\omega_{-1}}{d\sqrt{gh}}=-\frac{s}{a}. \tag{66}$$

For westerly gravity waves

$$\frac{d\omega_0}{d\sqrt{gh}} \approx -\frac{1}{2}\left[\frac{s}{a}+\frac{1}{2}\frac{2\sqrt{gh}\frac{s^2}{a^2}+4\beta}{\left(gh\frac{s^2}{a^2}+4\beta\sqrt{gh}\right)^{\frac{1}{2}}}\right]. \tag{67}$$

For easterly mixed gravity-Rossby waves

$$\frac{d\omega_0}{d\sqrt{gh}} \approx -\frac{1}{2}\left[\frac{1}{2}\frac{2\sqrt{gh}\frac{s^2}{a^3}+4\beta}{\left(gh\frac{s^2}{a^2}+4\beta\sqrt{gh}\right)^{\frac{1}{2}}}-\frac{s}{a}\right]. \tag{68}$$

For gravity waves

$$\frac{d\omega_n}{d\sqrt{gh}} \approx -\frac{2\sqrt{gh}\frac{S^2}{a^2}+(2n+1)\frac{2\Omega}{a}}{2\left[gh\frac{s^2}{a^2}+(2n+1)\frac{2\Omega}{a}\sqrt{gh}\right]^{\frac{1}{2}}}. \tag{69}$$

For Rossby waves

$$\frac{d\omega_n}{d\sqrt{gh}} \approx -(2n+1)\frac{2\Omega}{a}\frac{1}{gh}\frac{\frac{2\Omega}{a}\frac{s}{a}}{\left[\frac{s^2}{a^2}+(2n+1)\frac{2\Omega}{a}\frac{1}{\sqrt{gh}}\right]^2}. \tag{70}$$

We see from (66), (67), and (69) that growth rates for Kelvin and gravity waves will increase with increasing k $(=s/a)$ just as was the case in Section 2. However, we can also see from (68) and (70) that this is not so for mixed gravity-Rossby and Rossby waves. I shall study the above situation quantitatively later, but first I wish to discuss two important and related questions; namely, the nature of the finite-amplitude evolution of wave-CISK instabilities, and the effect of inhomogeneities in CISKability in latitude and longitude.

4. Finite-amplitude evolution of wave-CISK instabilities

Let us assume that initially we have an atmosphere in which z_t, z_c, z_b and α (which are presumably determined by the atmosphere's temperature and moisture distribution) are such that the atmosphere is unstable with respect to wave-CISK disturbances. Such disturbances will then proceed to grow exponentially (at least initially) until features of the physics which have not been included in the linear theory limit the finite-amplitude development of the disturbances. In some problems [i.e., Bénard convection (Joseph and Sattinger, 1972) and baroclinic instability (Pedlosky, 1970)] equilibration involves nonlinear terms in the wave fields. This does not appear to be the case for wave-CISK instabilities. At least observationally, tropical wave fields appear approximately linearizable. However, as we saw in Section 2b, wave-CISK instability, is, in general, accompanied by *mean* cumulus activity which will grow as the wave-CISK instabilities

grow. A likely mechanism for equilibration seems to be one in which the growing mean cumulus activity alters the temperature and moisture distribution of the atmosphere until values of z_c, z_t, α and z_b are reached for which the most unstable wave-CISK disturbances are neutral. To actually show how this occurs, one would need at least a cumulus parameterization which would describe the effect of cumulus activity on the detailed distribution of temperature and humidity, something which the crude parameterization of Section 2b does not do. It would probably also be necessary to calculate the mean meridional circulation induced by the mean cumulus activity (see Section 8). Clearly, the above equilibration calculation is beyond the scope of the present paper. However, I shall *assume* that such equilibration does occur, and that our atmosphere is, indeed, neutral with respect to the most unstable wave-CISK disturbances. From Section 2e we see that for typical ranges of z_c and z_t this implies that

$$L \approx 3 \text{ km}, \tag{71}$$

$$\alpha z_b \approx 0.4 \text{ km}. \tag{72}$$

Recalling that $L = 2\pi/\lambda$, it may be shown from Eq. (52) that (71) implies

$$h \approx 10 \text{ m}, \tag{73}$$

$$(gh)^{\frac{1}{2}} \approx 10 \text{ m sec}^{-1}. \tag{74}$$

The range of variation for L suggested by Fig. 4 is sufficiently small for us to adopt (73) as a constant. I pointed out in Section 2d that at the value of h given by (73) all appropriate wave-CISK disturbances will be neutral regardless of their horizontal wavenumbers (in this case given by n and s). Thus, wave-CISK establishes for the tropical atmosphere a second equivalent depth (i.e., $h \approx 10$ m), in addition to the usual equivalent depth for the free oscillation of the atmosphere, $h \approx 10$ km (*viz.* Lindzen, 1967). This second equivalent depth, it should be recalled, is largely determined by z_c.

Unlike the usual adiabatic free oscillations of the atmosphere which may have any magnitude within the constraints imposed by linearity, the overall magnitude of wave-CISK activity must be such as to maintain a neutral basic state. The determination of this magnitude calls for a finite-amplitude calculation with improved cumulus parameterization. Without going into such a calculation, it is nonetheless important to point out one important implication of the above situation. Namely, if one begins with one wave-CISK mode and excites a second mode, the amplitude of the first mode must diminish in order that the overall magnitude of wave-CISK activity remain the same. In general, if several modes are simultaneously present, some finite-amplitude calculation will also be necessary to determine the relative magnitudes of the various modes. Unfortunately, such calculations are beyond the scope of the present paper.

As noted in Section 2e, αz_b [as given by (72)] is about a factor of 4–6 smaller than observations suggest actually exists. On the face of it, this suggests that the atmosphere is highly unstable with respect to wave-CISK disturbances. But, as already mentioned, there are observational and theoretical reasons for not putting much emphasis on this point.

5. The effects of inhomogeneities in "CISKability"

"CISKability" requires a certain distribution of potential temperature with height, as well as air in the mixed surface layer which is sufficiently warm and moist. In general, CISKability exists over only a relatively small portion of the globe concentrated in the tropics. I shall represent CISKability by a function $f(\phi,\theta)$ [or $f(x,y)$], where $f(\phi,\theta)=1$ represents full CISKability. Over much of the globe $f(\phi,\theta)=0$, but it is possible for f to be between 0 and 1 if some CISKable regions have a smaller value of α than do other CISKable regions. It is also possible that z_c and z_t vary over the globe, but the parameterization of such variations would be more cumbersome (f would have to be a function of z). Fortunately, z_c and z_t seem to have rather restricted ranges of variation. The modification introduced by a non-constant f is simply as follows: the heating term in Eq. (47) must be multiplied by the projection of

$$f(\phi,\theta)\Theta_n(\theta)e^{is\phi}$$

on $\Theta_n(\theta)e^{is\phi}$. Since $f(\phi,\theta) \leqslant 1$, the projection must also be less than 1.

Let us first consider $f = f(\phi)$. Then we can write $f(\phi)$ as

$$f(\phi) = \bar{f} + \sum_{\substack{s=-\infty \\ s\neq 0}}^{\infty} f_s e^{is\phi}. \tag{75}$$

It follows immediately for this case that the projection of $f(\phi)\Theta_n(\theta)e^{is\phi}$ will simply be $\bar{f}$, the average value of $f(\phi)$; $\bar{f}$ can be associated with the parameter η in Section 2e. In general, the tropics are characterized by a high degree of horizontal homogeneity. However, if we assume that land surfaces are dry, $\bar{f}$ is reduced to 0.8 and a substantial contribution is made to the second term on the right-hand side of (75). In addition, there is evidence that small variations in surface temperature (on the order of 3C) substantially influence CISKability (Gray, 1968). Consistent with this, cloud climatologies (Sadler, 1969) show rather large areas of the tropics are almost always relatively cloud free. On the basis of the above, it seems possible that $\bar{f}$ might be as small as 0.2–0.4, in which case the critical value of αz_b for inviscid wave-CISK instability will be 1–2. This would substantially reduce the apparent instability noted in Section 4. Viscosity may also work in this direction.

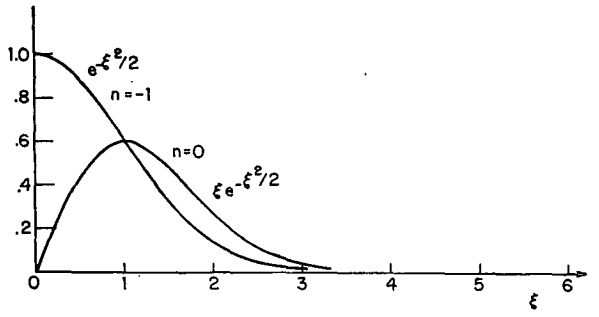

FIG. 8. Θ_{-1} and $\Theta_0(\xi)$. See text.

Without going into any further detail on this matter, I shall proceed on the assumption that the basic state of the atmosphere is neutral with respect to wave-CISK instabilities. The second term on the right-hand side of (75) will serve to force secondary waves, and as we shall see in Section 7, this has profound consequences. It should be emphasized that land-sea variations are sufficient to produce this secondary wave forcing.

The θ-dependence of f will also have some important consequences. Noting that CISKability is largely confined to the tropics, but that the equator itself appears dry, I will adopt a very simple model for f:

$$f(\phi,\theta)=f_1(\phi)f_2(\theta), \tag{76}$$

or, for an equatorial β-plane

$$f(x,y)=f_1(x)f_2(y), \tag{77}$$

where

$$\left.\begin{aligned} f_2(y)&=0, \quad |y|<y_e \\ f_2(y)&=1, \quad y_e\leqslant|y|\leqslant y_d \\ f_2(y)&=0, \quad |y|>y_d \end{aligned}\right\}. \tag{78}$$

I will assume $y_e\approx$O (150 km) and $y_d\approx$O (1500 km). These choices for f are made largely on the basis of simplicity. Although I shall retain them for this presentation, it is fairly clear that in regions like the Carribean $y_d\approx 2500$ km may be a more reasonable choice. The inclusion of such features, however, would call for expressions more complicated than (76). Using results for an equatorial β-plane, it is easily shown that the projection of $f(\phi,\theta)\Theta_n(y)e^{is\phi}$ is now

$$\tilde{f}_1\frac{\int_{\xi_e}^{\xi_d}\Theta_n^2(\xi)d\xi}{\int_0^{\infty}\Theta_n^2(\xi)d\xi}, \tag{79}$$

where

$$\xi=y\Big/\left(\frac{gha^2}{4\Omega^2}\right)^{\frac{1}{4}} \quad \text{[see. Eq. (55)]},$$

$$(\xi_e,\xi_d)=(y_e,y_d)\Big/\left(\frac{gha^2}{4\Omega^2}\right)^{\frac{1}{4}}.$$

Note that for $(gh)^{\frac{1}{2}}\approx 10$ m sec^{-1} [see Eq. (74)],

$$\left(\frac{gha^2}{4\Omega^2}\right)^{\frac{1}{4}}\approx 663 \text{ km}, \tag{80}$$

and, hence, for $y_d\approx 1500$ km, $\xi_d\approx 2.26$, and for $y_e\approx 150$ km, $\xi_e\sim 0.226$.

From (79) we see that the greater the magnitude of Θ_n outside $\xi_e<|\xi|<\xi_d$, the smaller the projection will be and the more stable the particular mode will be. Moreover, from Lindzen (1967; Fig. 4 of that paper) we see that, for a given $(gh)^{\frac{1}{2}}$, the latitudinal extent of Θ_n will increase as n increases. Thus, we may expect stability to increase with increasing n, i.e., we expect only waves with small n's to be produced by wave-CISK. However, the crudeness with which I have specified $f(\phi,\theta)$ also suggests that we ought to be cautious about attributing different stabilities to modes with only slightly different projections. Thus, for example, from Fig. 8 which shows $\Theta_{-1}(\xi)$ and $\Theta_0(\xi)$ we see that both modes should have similar projections and similar stability properties. For higher order modes [for which $\Theta_n(\xi)$ depends on wave type and s] the situation becomes somewhat more arbitrary. Fig. 9 shows $\Theta_1(\xi)$ and $\Theta_2(\xi)$ for Rossby waves with various values of s. As concerns projections, the dependence on s does not appear profound. The projection of Θ_1 appears as though it might be somewhat smaller than for the $n=-1$ and $n=0$ modes, but not sufficiently smaller for the difference in the condition for neutral stability to be very meaningful. On the other hand, the projection for the Θ_2 Rossby wave seems substantially smaller than for the Θ_1 mode; hence, if we assume that the $n=-1$, $n=0$ and the $n=1$ Rossby modes are neutrally stable, the $n=2$ Rossby modes will be stable (i.e., they will decay with time). Fig. 10 shows Θ_1 and Θ_2 for *easterly* gravity waves. These modes show a marked dependence on s. For very small values of s, these modes appear to have smaller projections than the $n=-1$ and $n=0$

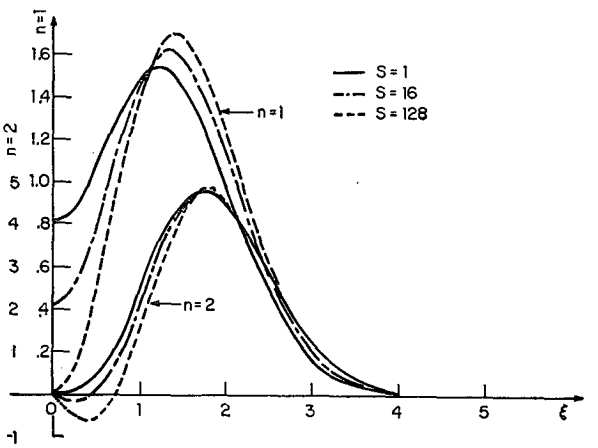

FIG. 9. $\Theta_1(\xi)$ and $\Theta_2(\xi)$ for Rossby waves at several different values of zonal wavenumber s. See text.

modes, and therefore ought to be stable (though the matter may be questionable for $n=1$). However, for large values of s, Θ_1 and Θ_2 for easterly gravity waves approach Θ_{-1} and Θ_0; therefore, $n=1$ and $n=2$ easterly gravity waves ought to be neutrally stable for large values of s. Finally, in Fig. 11, I show Θ_1 and Θ_2 for *westerly* gravity waves. The s-dependence of these modes is not profound and, in general, $n=1$ and $n=2$ westerly gravity waves appear to have smaller projections than the $n=-1$ and $n=0$ modes. Hence $n=1$ and $n=2$ westerly gravity waves ought to be stable (again, with some room for doubt on $n=1$). Presumably all modes for $n>2$ ought to be stable.

In summary, when the latitude variation of CISKability is taken into account, then $n=-1$ (Kelvin wave) modes, $n=0$ modes and $n=1$ (Rossby wave) modes, and $n=1$ and $n=2$ (easterly gravity wave) modes at large values of s, appear to have similar stability properties. In particular, when the atmosphere is neutrally stable with respect to these modes, it should be stable with respect to all other modes. Thus, in studying the detailed dispersive properties of wave-CISK disturbances, I will restrict myself to the above mentioned modes. It must, however, be recalled that this restriction is based on our simplified choice of $f(\theta,\phi)$. More generally, we can say that CISKability *does* cease outside the tropics so that there will always exist some N such that for $n>N$ the modes will be stable. For purposes of this paper the precise cutoff is not important.

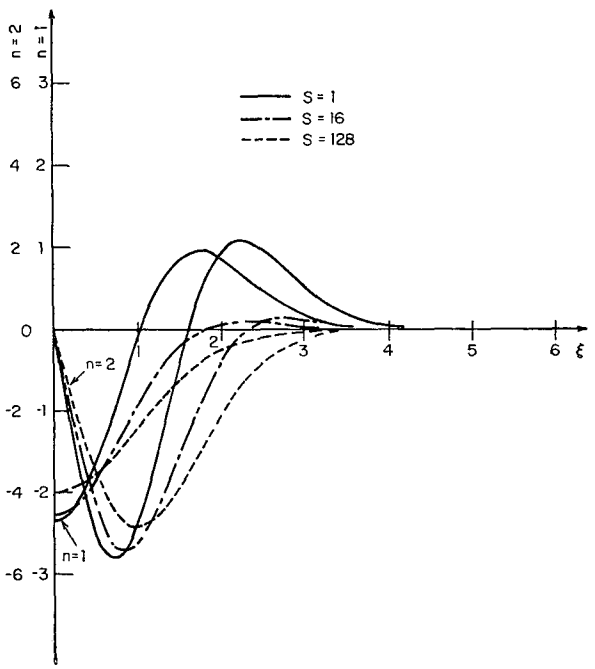

FIG. 10. $\Theta_1(\xi)$ and $\Theta_2(\xi)$ for easterly gravity waves at several different values of zonal wavenumber s. See text.

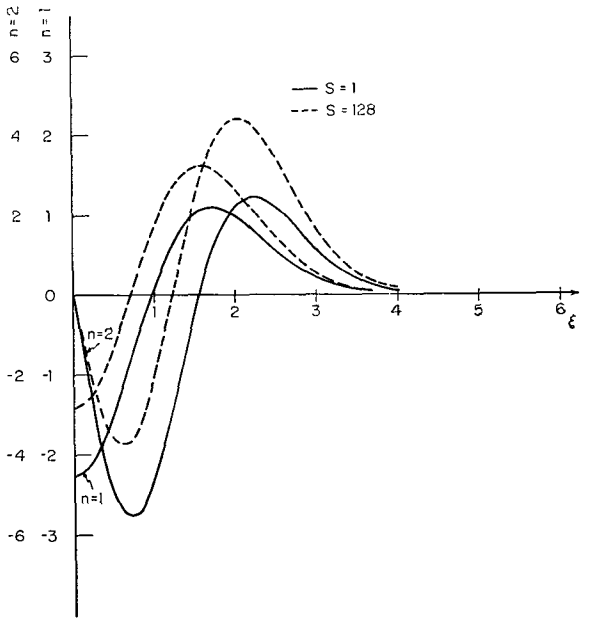

FIG. 11. $\Theta_1(\xi)$ and $\Theta_2(\xi)$ for westerly gravity waves at several different values of zonal wavenumber s. See text.

In Section 8 an additional aspect of the latitudinal inhomogeneity of CISKability will be discussed.

6. Detailed dispersive and stability properties: Preferred modes

As explained in Section 4, I expect the mean cumulus activity associated with wave-CISK instabilities to produce a neutrally stable configuration of z_c, z_t, α and z_b, where the equivalent depth for the neutral disturbances will be $h\approx 10$ m. Moreover, in Section 5 I showed that due to latitude variations in CISKability, the neutral stability of the atmosphere with respect to modes with small n's (meridional wavenumber on an equatorial β-plane) implies its stability with respect to modes with larger n's.

If we take $h\approx 10$ m, then Eqs. (53), (56), (57), (59) and (60) give us the frequency of neutral modes as a function of s. This dependence for $n=-1$ westerly Kelvin waves, $n=0$ westerly gravity waves, $n=0$ easterly mixed gravity-Rossby waves, $n=1$ easterly Rossby waves, and $n=1$ and $n=2$ gravity waves is shown in Fig. 12 where the period ($|2\pi/\omega|$) is plotted as a function s. If, in fact, the atmosphere is slightly unstable, then the e-folding time for unstable disturbances will be proportional to $[d\omega/d(gh)^{\frac{1}{2}}]^{-1}$ evaluated at the neutral value of $(gh)^{\frac{1}{2}}$ (see Section 3). Formulas for this quantity are given by (66)–(70), and its value as a function of s for various modes is shown in Fig. 13. The results shown in Fig. 13 ignore the latitude variation of CISKability; when this is taken into account, the results in Fig. 13 for $n=1$ and $n=2$ gravity waves are only valid for easterly waves with large values of s; westerly waves and easterly waves with small values of

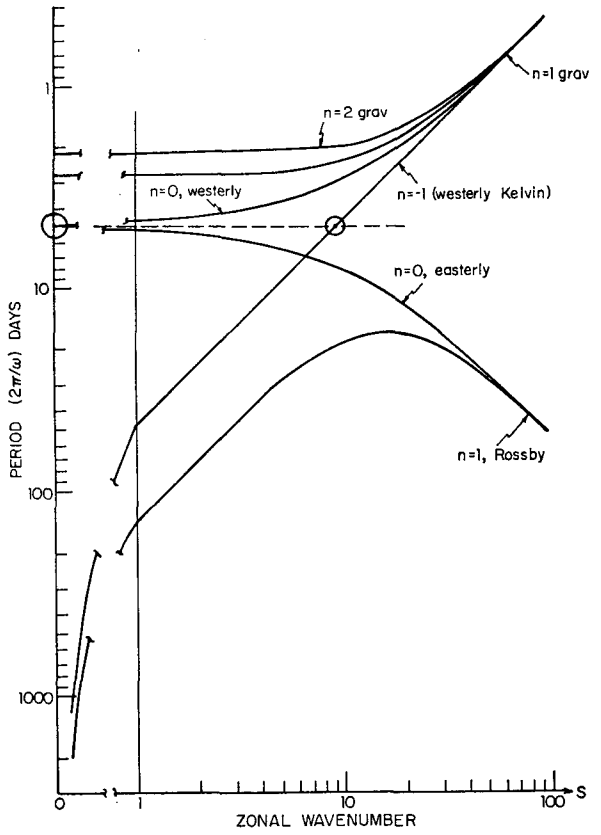

FIG. 12. Wave period as a function of zonal wavenumber for various wave types under conditions of neutral stability.

s should be stable (see Section 5). The results shown in Fig. 13 are essentially those reported by Hayashi (1970). The most rapidly growing disturbances are the Kelvin waves, westerly $n=0$ waves, and easterly $n=1$ and 2 gravity waves, all at large values of s. In general, the $n=0$ westerly waves grow more rapidly than either the $n=0$ easterly waves or the $n=1$ Rossby waves. For $s<9$ the $n=0$ easterly waves grow more rapidly than any of the $n=1$ Rossby waves, though for $s>9$, the $n=1$ Rossby waves grow more rapidly than the $n=0$ easterly mixed gravity-Rossby waves. However, if we take the view that the effect of the instabilities is to produce a neutrally stable basic state, then *all* the disturbances to which the atmosphere was unstable will now be neutral "free" oscillations. Under these circumstances the smaller wavenumbers will play a prominent role since the natural sources of disturbances (orography, mid-latitude disturbances) are dominated by smaller values of s. The question is what principles determine which modes, if any, are preferentially excited. Although I cannot answer this question, at this time, there does exist one mode, the $n=0$ mode for which $s=0$, the consequences of whose existence are particularly interesting for tropical meteorology. In this and subsequent sections I will investigate these consequences. As we shall see, the assumption that the $n=0$, $s=0$ mode exists to a significant extent leads to a remarkably coherent picture of tropical meteorology in general. Although the prominence of the $n=0$, $s=0$ mode is conjectural at this stage, there are, in fact, a number of qualitative reasons which suggest the plausibility of the conjecture:

(i) Under unstable conditions, the $n=0$, $s=0$ mode is comparably unstable with any other modes at small values of s; this, however, is probably unimportant if my assumption of neutral stability is correct.

(ii) More important is the fact that this is, probably, the *only* viable wave-CISK mode having a finite frequency at $s=0$. Those modes for which $s=0$ are, to a high degree of approximation, unaffected by the mean zonal wind. Thus, their frequency, as observed at the ground, will be *invariant* under variations of zonal wind. Even if other free oscillations (corresponding to $h\approx 10$ m) exist, the frequencies of the $s=0$ modes will appear as rather narrow lines in power spectra. In addition, it should be noted that the $n=0$, $s=0$ mode is the only

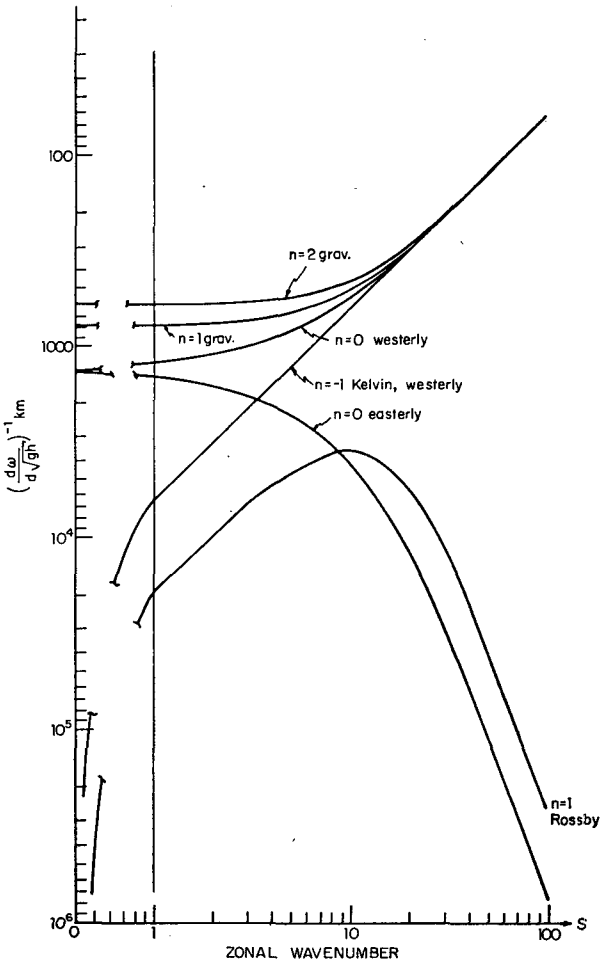

FIG. 13. The proportionality factor $[(d\omega)/d(gh)^{\frac{1}{2}}]$ for the e-folding time as a function of s for various wave types under slightly unstable conditions.

possible long-period, free-standing oscillation. Free-standing oscillations for other values of s will be impossible because for any choice of $s \neq 0$, easterly and westerly waves on a rotating atmosphere will behave differently. Of course, longitudinal inhomogeneities in CISKability will make an $n=0$, $s=0$ mode appear to be associated with $s \neq 0$ at least in cloud photographs.

(iii) Related to (ii) is the likelihood that modes for which $s \neq 0$ will actually be inhibited. When $s \neq 0$, the frequencies shown is Fig. 12 correspond to frequencies measured by observers moving with the mean zonal flow. But, it is observed that the mean zonal flow in the tropics varies substantially with longitude (Palmén and Newton, 1969). Under these conditions, it is difficult to envisage how coherent modes of the sort envisaged in a normal mode analysis can set on unimpeded unless $s=0$ (when $s=0$ there is no Doppler shifting by the mean zonal flow). These considerations are *not* likely to apply for very *large* values of s, since the zonal scale of these modes will be so small that the modes will not "see" the longitude variations of the mean zonal flow. We will have to consider this matter in some detail in Sections 7 and 9.

The conjectured importance of the $n=0$, $s=0$ mode has a number of implications for the meteorology of the tropics. First, we would expect that the period of this mode would be a prominant feature of the time behavior of the tropics. From Fig. 12, we see that this period is $\sim$4.8 days, and it has long been noted that this period does, in fact, dominate much of tropical meteorology (Wallace, 1971). Moreover, since $s=0$, we would expect that this period would be manifested, at least in part, by a pulsation in place of cumulus convection with a period of $\sim$4.8 days. Such an oscillation has been found by Wallace in satellite cloud photographs, and is readily visible in the cloud photographs presented by Chang (1970). Other consequences require somewhat more detailed discussion.

7. Interaction of the $n=0$, $s=0$ mode with other waves

The $n=0$, $s=0$ mode will tend to force, through interaction with the zero-average part of $f(\phi)$ [i.e., the second term on the right-hand side of (75)], a spectrum of waves having the zonal wavenumbers involved in $f(\phi)$ and the period (as measured by a stationary observer) of the $n=0$, $s=0$ mode (i.e., $\sim$4.8 days). Such a mechanism has already been invoked by Holton (1972) to account for the observed 5-day waves in the tropical stratosphere—without, however, accounting for the assumed 5-day pulsation of the cumulus heating. The tropospheric response to the above forcing may be expected to be particularly strong when the forced wave is also a possible neutral wave-CISK mode[4] since in such cases we will have resonant excitation. From Fig. 12 we see that in the absence of any mean zonal flow, this will be the case for Kelvin waves with $s \approx 9$–10. However, when there is a mean zonal flow[5], then the periods shown in Fig. 12 are periods measured by an observer moving with the mean flow while resonant forcing will occur when the period as measured by a stationary observer is $\sim$4.8 days. If ω is the frequency observed in the moving frame (and $|2\pi/\omega|$ the period), then the period observed in a stationary frame will be

$$\tau_{\text{stationary}} = \left| \frac{2\pi}{\omega - k u_0} \right|. \tag{81}$$

Thus, the stationary observer will measure reduced periods for easterly waves ($\omega/k > 0$) in easterly flows ($u_0 < 0$), and increased periods for easterly waves in westerly flows. The extreme for the latter effect will occur when $\omega = k u_0$ and the stationary observer measures an infinite period; if u_0 is increased further so that $u_0 > \omega/k$, then the easterly wave will appear to the stationary observer as a westerly wave whose period, $\tau_{\text{stationary}}$, will decrease as u_0 increases. The above effects are reversed in the obvious manner for westerly waves. The nature of the above effects is seen in Fig. 14 where $\tau_{\text{stationary}}$ is shown as a function of s for the $n=1$ Rossby wave and several different values of u_0. Although there is no resonant forcing for $u_0=0$, any finite u_0 will involve resonant forcing at some value of s; for very small u_0's, however, this may involve unrealizably large values of s. This is not necessarily the case for gravity wave modes whose phase speeds may exceed u_0 at all values of s; in that case u_0 will not usually lead to resonant forcing. Fig. 15 shows the value of s at which resonant forcing takes place as a function of u_0 for $n=-1$ westerly Kelvin waves, $n=0$ easterly mixed gravity-Rossby waves, $n=0$ westerly gravity waves, and $n=1$ easterly Rossby waves. For the $n=0$ westerly gravity waves we see that resonant forcing occurs only when $u_0 < -5$ m sec^{-1}. For a typical value of zonal wind in the tropics, $u_0 = -3$ m sec^{-1}, we see that there will be resonant forcing for Kelvin waves at $s=14$ (wavelength $\sim$2872 km), for $n=0$ mixed gravity-Rossby waves at $s=18$ (wavelength $\sim$2234 km) and for $n=1$ Rossby waves at $s=24$ (wavelength $\sim$1676 km). The last two disturbances are easily identified with the observed easterly waves of the tropical troposphere whose wavelengths are typically 1000–3000 km but whose periods are usually $\sim$5 days [a review of observed tropical waves may be found in Wallace (1971)]. Two important conclusions can be drawn from the above discussion. First, easterly waves of the sort observed in the tropics *necessarily accompany* the existence of the $n=0$, $s=0$

[4] This will not be the case above $z=z_t$ for reasons given at the end of section 2e; namely, the amplitude of neutral wave-CISK modes is very weak for $z > z_t$ due to interference effects.

[5] For simplicity, I will assume such a flow to be independent of y and z, though for reasons discussed in Section 2e I expect that the magnitude of such a flow below $z=z_c$ will be of primary importance.

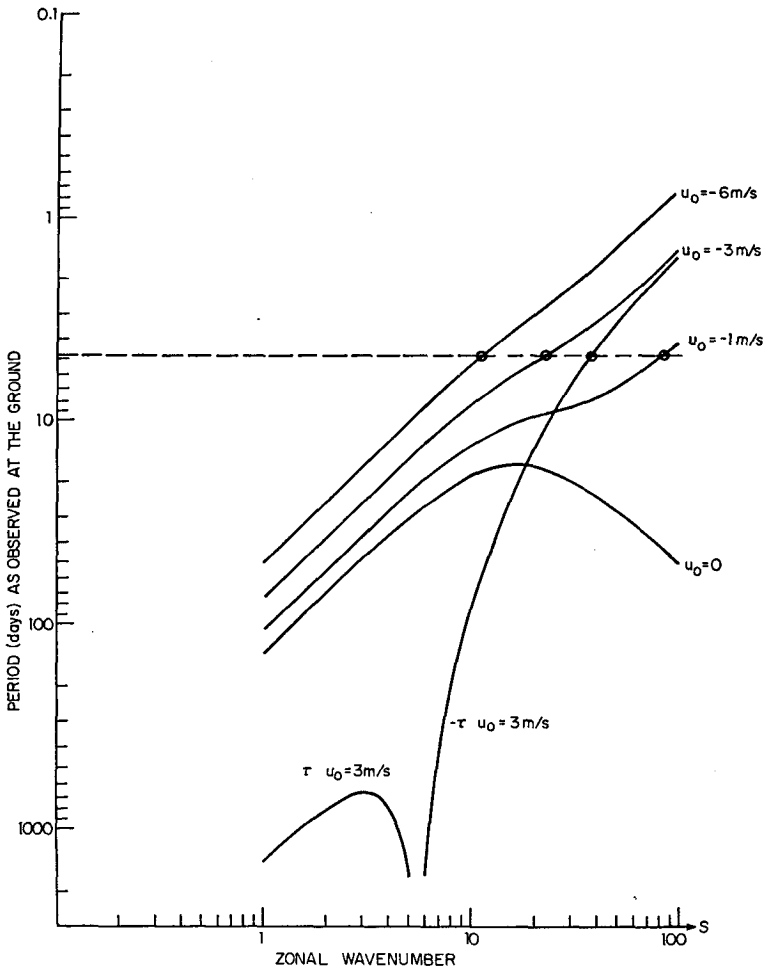

FIG. 14. The period observed at the ground for $n=1$ neutral, wave-CISK Rossby waves in atmospheres with various mean zonal flows u_0.

wave-CISK mode even if the only inhomogeneity in CISKability arises from land-sea variations. Second, we see that for a ground-observed period of 5 days, wave-CISK modes have the horizontal scales of observed tropical, tropospheric waves. This last conclusion is independent of the existence of the $n=0$, $s=0$ mode, and argues strongly for the existence of a tropical equivalent depth of O (10 m).[6]

As already noted, the wavelength of resonantly forced Rossby and mixed gravity-Rossby CISK waves decreases to zero as $|u_0| \to 0$. Now, for Rossby type waves of finite amplitude, the importance of nonlinear terms in the equations of motion (which I have neglected in my analysis) will increase as wavelength decreases. It is highly speculative to suggest, but not inconceivable, that the diminishing scale of resonantly forced Rossby CISK waves as $|u_0| \to 0$ and the consequently increasingly important nonlinear effects (including enhanced boundary layer pumping due to relative vorticity) could lead to the development of cutoff, isolated vortices which we associate with intense tropical storms (i.e., hurricanes). This is currently being investigated with Mr. Lloyd Shapiro at Harvard.

Finally, I wish to point out that the $n=0$, $s=0$ mode interacting with the zero average part of $f(\phi)$ can also resonantly force non-CISK free oscillations of the atmosphere (i.e., oscillations for which $h \approx 10$ km rather than 10 m), and this may account for the $n=1$, $s=2$ Rossby wave, observed by Madden and Julian (1972b), whose period observed at the surface is ~ 5 days. In general, though, these non-CISK waves will have a global extent, and hence their forcing by the $n=0$, $s=0$

[6] Prof. J. R. Holton has privately pointed out that additional support for the existence of a 10 m equivalent depth in the tropics comes from the 40–50 day wave observed by Madden and Julian (1972a). The wave they observed resembles, in its horizontal structure, an $s=1$ Kelvin wave. As we see from Fig. 12, the $s=1$ Kelvin wave in an atmosphere with an equivalent depth of 10 m does have a period of about 40–50 days. Of course this is the period observed moving with the mean zonal flow. However, in the region where the 40–50 day wave is observed (Indian Ocean, western Pacific), the mean zonal flow near the surface is rather small—certainly much smaller than the Kelvin wave phase speed of 10 m sec^{-1}.

wave-CISK mode will be relatively weak. However, damping may also be small for these modes.

8. Wave-CISK and the ITCZ's

As pointed out in Section 2b, wave-CISK disturbances are associated with *mean* cumulus heating. Thus, wave-CISK disturbances serve to pump latent heat into the upper troposphere, where this mean heating can force the Hadley circulation. If all tropical latitudes were equally CISKable, then the mean cumulus heating would have the same distribution with latitude as does the magnitude of w for the superposition of the various wave-CISK disturbances. If we further restrict ourselves, for the moment, to the $n=0$, $s=0$ mode, then Fig. 8 shows that maximum $|w|$ and, hence, maximum mean cumulus heating occur for $\xi=\pm 1$ [or using Eq. (80), at $y=\pm 663$ km]. These are, in fact, very close to the values of y most commonly associated with the observed intertropical convergence zones (ITCZ's). Unfortunately, the real situation cannot be quite so simple.

First, in all likelihood, all tropical latitudes are not equally CISKable and mean cumulus heating will therefore not have the same distribution with latitude as does the magnitude of w. It should be emphasized that it is not at all essential to wave-CISK that the horizontal distributions of $w(z_b)$ and cumulus heating coincide; it is only necessary that the latter have a finite Fourier projection on the former. Indeed, from the discussion of Sections 2e and 4, it would appear necessary for wave-CISK neutrality that the projections be appreciably less than 1. As an example of this effect consider a situation where latitudes north of the equator are CISKable while those south of the equator are not. An $n=0$, $s=0$ mode would then give rise to a maximum of cumulus heating at $\xi=+1$ and no heating at $\xi=-1$; the projection of this heating on the $n=0$, $s=0$ mode (ignoring longitudinal variability in CISKability) is $\frac{1}{2}$. From observations analyzed by Gray (1968) among others it appears that for much of the year sea surface temperatures in both the Atlantic and Pacific are considerably colder south of the equator than north of the equator. Thus, the above example may be relevant to reality.

Second, we cannot restrict ourselves to the $n=0$, $s=0$ mode. As I have shown in Section 7, such a mode will necessarily be accompanied by resonantly excited 5-day traveling waves. Those traveling waves for which $n=0$ will have the same latitude distribution of $|w|$ as does the $n=0$, $s=0$ mode. However, $n=-1$ Kelvin waves will tend to have maximum $|w|$ at the equator while Rossby waves with $n\geq 1$ will have maximum $|w|$ at $|\xi|>1$. The relevant $|w|$ arises from the superposition of the above waves. Although the prominance of the $n=0$, $s=0$ mode may lead to $\xi=\pm 1$ being the sites of maximum $|w|$ on the average, it is clear that there will be periods and longitudes when maximum $|w|$ occurs

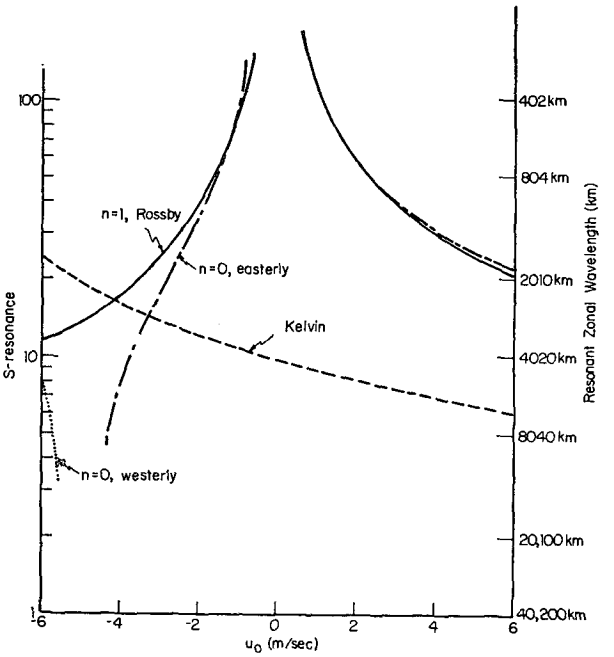

FIG. 15. The wavenumber s at which various waves have a period of ~4.8 days as observed at the ground, as a function of mean zonal flow.

elsewhere. This, too, is consistent with the observed variability in the position of the ITCZ. The theoretical prediction of this position would require a knowledge of the relative magnitudes of the various modes, and, as mentioned in Section 7, the determination of relative magnitudes is beyond the scope of the present work.

Third, a knowledge that maximum mean cumulus heating is occurring at those latitudes at which the ITCZ is observed does *not* immediately determine the structure of the ITCZ or the associated Hadley circulation. To determine these matters one must calculate the mean circulation forced and the mean heating produced by wave-CISK.[7]

Such an approach to the ITCZ differs rather profoundly from the stability type approaches to the ITCZ used by Charney (1971a), Bates (1970) and others. In these approaches the cumulus heating is forced by the boundary layer pumping (i.e., Ekman pumping) due to the mean circulation produced by the same cumulus heating. In the present work the mean cumulus heating is due to the presence of the $n=0$, $s=0$ wave-CISK mode and its associated low-level convergence. The mean cumulus heating, therefore, is largely independent of both surface friction and the Hadley circulation. In fact, in the absence of friction one might reasonably expect the response to mean heating to be such that the temperature adjusts itself until the cumulus heating is balanced by infrared cooling while the circulation will

[7] While such calculations are beyond the scope of the present paper, Mr. E. Schneider, at Harvard, is carrying out such calculations, and will report them in due course.

consist in a zonal thermal wind in balance with the temperature distribution and *no* meridional Hadley circulation. When friction is included there will have to be some meridional circulation in response to the heating (Charney, 1971b; Lindzen, 1968), but for normally expected eddy viscosities [O (10^5 cm^2 sec^{-1})] the frictional effects will be primarily restricted to boundary layers; and since the cumulus heating is found well above the surface, one may expect the Ekman pumping (and hence *mean* low-level mass convergence as well) to be weak, and that, as a result, infrared cooling will continue to be the process primarily balancing the cumulus heating. If the adiabatic cooling and thermal advection associated with an Hadley circulation are to be significant in balancing cumulus heating, then we must have strong internal, upper level friction. Holton and Colton (1972) have discovered evidence that such friction does exist near 200 mb, and that this friction is probably due to cumulus convection.[8] With such friction, I would expect a meridional circulation which would involve downdrafts not only at high latitudes but over the equator as well [just as in Bates' (1970) model]. The downdrafts over the equator should dry the equator, consistent with the observation of a dry equatorial zone. It is also conceivable (though explicit calculations will be needed to determine the matter) that the regions of updraft centered at $\xi=\pm 1$ will be much narrower than the latitudinal extent of the heating. It is my impression that the reason stability-type calculations imply maximum growth for an infinitesimally narrow ITCZ is as much due to the fact that they require heating and circulation to have the same width as to the details of the assumed cumulus parameterization.

As I have already noted, if the above picture of the Hadley circulation consisting in the response to the mean upper level cumulus heating (due to low-level wave convergence) in the presence of internal upper level friction is correct, then the contribution of the mean circulation to $w(z_b)$ (see Section 2) should be small. It should also be noted that the Hadley circulation (including the ITCZ's) forced by the mean heating associated with wave-CISK modes, is *not*, itself, a wave-CISK mode. It will be a simple, thermally forced meridional circulation without the detailed vertical structure characterizing the waves.

9. Interaction of the $n=0$, $s=0$ and other long-period modes with cloud clusters

As noted in Sections 6 and 7 (see Fig. 12 in particular) I expect wave-CISK to lead to an $n=0$, $s=0$ mode as well as Rossby waves, though if some source of disturbance were present I would expect gravity waves with very large wavenumbers to be present as well—at least on a local basis. In this Section I wish to show that the joint presence of the long-period modes and high-wavenumber gravity waves alters the above picture in an important way. Note from Fig. 12 that not only are the spatial scales (as measured by s) extremely different for these two types of waves, but so too are their time scales (several hours vs 4.8 days). Thus, the very short waves will "see" the long-period modes as their "mean" environment, and in this instance, the "mean" environment will, indeed, have a significant upward $w(z_b)$ during half of each 4.8 days; a downward, cumulus-inhibiting $w(z_b)$ will exist during the other half. If αz_b is such that the long-period modes are *neutrally* stable, then we see from Section 2b that the "mean" state presented by the long-period modes in the regions where $w(z_b)>0$ will be unstable to high wavenumber gravity waves, since for these waves the α in αz_b must [due to the pre-existence of a $w(z_b)$] be replaced by 2α; at the same time, the high-wavenumber gravity waves will contribute nothing to the mean cumulus heating. The above situation will continue until the amplitude of $w(z_b)$ due to the gravity waves exceeds $w(z_b)$ due to the long-period modes, at which point the growth rate of the gravity waves will decrease and they will begin contributing to the mean cumulus heating. However, I don't think that this last mentioned situation will be fundamentally important since the time over which the high-wavenumber disturbances may grow is limited to half of the period (i.e., $\sim$2.4 days) and even during this time, it is only when $w(z_b)$ is a maximum that conditions for the large-scale growth of the high-wavenumber gravity waves is optimal.

From Fig. 13, we see that, according to my calculations, the instability of high-wavenumber gravity waves will tend to select zero ($s=\infty$) as the preferred scale. This rather unreasonable result comes about from our implicit assumption that cumulus convection and heating equilibrates with $w(z_b)$ instantaneously. In reality, the life cycle of a hot tower takes on the order of an hour, and as a result I would not expect that wave-CISK instability would prove effective for waves whose time scales (ω^{-1}) are <O (2 hr). Now for large values of s,

$$\omega^2 \approx ghk^2, \tag{82}$$

(where $k=s/a$) for the gravity waves, or equivalently,

$$|\omega| \approx (gh)^{\frac{1}{2}}|k|. \tag{83}$$

If, for $|\omega|^{-1}$ we take 2 hr, and for h, 10 m, we see that

$$|k| \approx 13.9\times 10^{-3}\ \text{km}^{-1},$$

which implies an horizontal wavelength ($L=2\pi/k$),

$$L \approx 452\ \text{km}. \tag{84}$$

Half of L (i.e., 226 km) is indeed a typical observed scale for cloud clusters! It thus appears that the long-period modes *must* be modulated by cloud clusters for which the long-period modes provides an unstable

[8] N. B. Strong friction localized near the top of cumulonimbus towers is unlikely to affect wave-CISK results since the short vertical scale of wave-CISK modes makes their behavior below $z=z_c$ fairly insensitive to what is going on near z_t (see Section 2e).

environment (during half of their period). The interesting possibility arises that more wave-CISK disturbance energy might be released by the joint instability of long- and short-period modes than by the instability of short-period gravity waves alone.

10. Conclusion

I have, in this paper, undertaken a study of CISK where the low-level convergence is due to internal waves (wave-CISK) rather than Ekman pumping. I find that wave-CISK is indeed possible, with the most unstable wave-CISK modes having vertical wavelengths such as to approximately maximize subcloud convergence. This leads to vertical wavelengths of O (3 km). Associated with wave-CISK modes, there is always mean cumulus heating. The last effect arises simply because there are no negative clouds. I suggest that the mean cumulus activity associated with wave-CISK acts to alter the basic state in such a way as to leave it neutral with respect to wave-CISK. For an unstable basic state some wave-CISK modes grow more rapidly than others; however, when the basic state is neutral, it is simultaneously neutral for all horizontal wavenumbers. Thus, under neutral conditions *wave-CISK provides the tropical atmosphere with an equivalent depth of O (10 m)* in addition to the usual equivalent depth of O (10 km). Several consequences follow from the existence of such a small equivalent depth:

1) The existence of a detailed vertical structure characteristic of observations by Madden and Zipser (1970).
2) The existence of solutions to Laplace's tidal equation which are confined to the tropics.
3) The existence of Rossby-type equatorial waves which, for observed near surface mean zonal flows, have 5-day periods (as measured by a stationary observer) and zonal wavelengths of O (2000 km) consistent with observed easterly waves.
4) The existence of a 50-day, $s=1$, Kelvin wave similar to the disturbance observed by Madden and Julian (1971a).
5) The existence of a longitude-independent (i.e., the zonal wavenumber, s, is zero), antisymmetric standing oscillation with a period of about 5 days.

Although the observational basis for the last item is limited (Wallace, 1971), its existence is of potentially great importance for tropical meteorology for the following reasons:

(i) The $n=0$, $s=0$ oscillation is the only theoretically possible long period standing oscillation.

(ii) Modes for which $s=0$, are largely unaffected by the mean zonal flow and its longitudinal variation since they are not Doppler-shifted; thus, the period of the $n=0$, $s=0$ mode (i.e., 5 days) will appear as a line in tropical spectra.

(iii) Due to inhomogeneities in surface conditions, the $n=0$, $s=0$ oscillation will resonantly force the 5-day traveling waves described in consequence 3) above. As shown in Section 7, this also may have implications for the transition from an easterly wave to a hurricane.

(iv) The $n=0$, $s=0$ oscillation can give rise to maximum mean cumulus heating at the latitudes which are generally held to be the most common positions for ITCZ's (i.e., at $\pm 6°$).

(v) The $n=0$, $s=0$ oscillation will force 5-day standing pulsations in cumulus activity of the sort invoked by Holton (1972b) to explain the origin of stratospheric easterly waves.

All of the above have been discussed at length in the body of this text.

Finally, I have shown that all long-period wave-CISK modes are themselves unstable with respect to short period [O (10 hrs)], "cluster" scale [O (200 km)] wave-CISK gravity waves.

Clearly, a great deal more detailed theoretical work is needed to establish the above results and implications more firmly. In particular, the long-period and short vertical scale of many of the above modes suggests an important role for viscosity though the precise nature of the role is difficult to specify *a priori*. On the one hand, viscosity serves to inhibit the downward propagation of waves from the cumulus heating region thus diminishing low-level convergence and, in consequence of this, CISK effectiveness; on the other hand, for Rossby-type waves, Ekman pumping enhances low-level convergence. Preliminary calculations, which will be described separately, suggest that the net effect of viscosity is generally to diminish CISK effectiveness. It also appears that, for long-period oscillations, viscosity tends to reduce the vertical variability implied by Figs. 4 and 5.

Apart from viscosity, it will also be necessary to consider finite-amplitude effects, and associated with this, better cumulus parameterizations, in order to determine the magnitude of wave-CISK activity and partition of energy among the various possible modes.

Nevertheless, I hope that this paper may prove useful in providing the beginning of an integrated view of tropical meteorology. This work, even in its present form, provides a substantial number of predictions which should be amenable to observational checks during the forthcoming GATE (GARP Atlantic Tropical Experiment) program.

Acknowledgments. This work has been supported by Grant GA3390X from the National Science Foundation. I also wish to acknowledge the aid of Messrs. E. Schneider and L. Shapiro whose frequent questions prodded me into thinking about many of the items discussed in this paper.

Finally, I wish to thank Prof. Richard J. Reed for reading an earlier version of this paper and making useful comments.

APPENDIX A

Thermally Forced Vertical Structure

The Green's Function for Eq. (12) satisfies the equation

$$\frac{d^2G(z,z_0)}{dz^2}+\lambda^2G(z,z_0)=\delta(z-z_0), \tag{A1}$$

where $\delta(z)$ is a delta function. The boundary conditions for $G(z,z_0)$ are

$$\left.\begin{aligned} G(z,z_0)&=0, \quad \text{at} \quad z=0 \\ G(z,z_0)&=Ae^{-i\lambda z}, \quad z>z_0 \end{aligned}\right\}.$$

While $G(z,z_0)$ is taken to be a continuous function, (A1) requires that

$$\left.\frac{dG}{dz}\right|_-^+=1, \quad \text{across} \quad z=z_0. \tag{A2}$$

Solutions to (A1) are of the form

$$\left.\begin{aligned} G&=Ae^{-i\lambda z}, \quad z>z_0 \\ G&=B\sin\lambda z, \quad z<z_0 \end{aligned}\right\}.$$

Continuity and (A2) at $z=z_0$ then yield

$$\left.\begin{aligned} B&=\frac{1}{\lambda}e^{-i\lambda z_0} \\ A&=\frac{1}{\lambda}\sin\lambda z_0 \end{aligned}\right\}.$$

Thus,

$$G(z,z_0)=\begin{cases} \dfrac{1}{\lambda}\sin\lambda z_0 e^{-i\lambda z}, & z>z_0 \\ \dfrac{1}{\lambda}e^{-i\lambda z_0}\sin\lambda z, & z<z_0 \end{cases} \tag{A3}$$

Now if we have an equation

$$\frac{d^2\tilde{w}}{dz^2}+\lambda^2\tilde{w}=f, \tag{A4}$$

where $\tilde{w}(0)=0$, and if $f=0$ for $z>z_t$, and $\tilde{w}\propto e^{-i\lambda z}$, $z>z_t$, then we may express $\tilde{w}$ in terms of $G(z,z_0)$ as

$$\tilde{w}(z)=\int_0^\infty G(z,z_0)f(z_0)dz_0, \tag{A5}$$

$$=-e^{-i\lambda z}\int_0^z\frac{\sin\lambda z_0}{\lambda}f(z_0)dz_0 - \frac{\sin\lambda z}{\lambda}\int_z^\infty e^{-i\lambda z_0}f(z_0)dz_0. \tag{A6}$$

If $f=0$ for $z<z_e$ and $z>z_t$, then (A6) reduces to (15).

REFERENCES

Arakawa, A., 1971: Parameterization of cumulus convection (Lecture notes distributed at a Workshop of the UCLA General Circulation model). To be published in Numerical Simulation of Weather and Climate, Tech. Rept. No. 7, Dept. of Meteorology, UCLA.

——, and W. Schubert, 1974: Interaction of a cumulus cloud ensemble with the large-scale environment, Part I. *J. Atmos. Sci.*, **31**, (in press).

Bates, J. R., 1970: Dynamics of disturbances on the intertropical convergence zone. *Quart. J. Roy. Meteor. Soc.*, **96**, 677–701.

Chang, C. P., 1970: Westward propagating cloud patterns in the tropical Pacific as seen from time-composite satellite photographs. *J. Atmos. Sci.*, **27**, 133–138.

Chandrasekhar, S., 1961: *Hydrodynamic and Hydromagnetic Stability*. Oxford, Clarendon Press, 625 pp.

Chapman, S., and R. S. Lindzen, 1970: *Atmospheric Tides*. Reidel, Dordrecht, Holland, 200 pp.

Charney, J. G., 1971a: Tropical cyclogenesis and the formation of the intertropical convergence zone. *Lectures in Applied Mathematics*, Vol. 13, Providence, R. I., Amer. Math. Soc., 355–368.

——, 1971b: Planetary fluid dynamics (Lecture notes). Dept. of Meteorology, M.I.T., Cambridge, Mass.

——, and A. Eliassen, 1964: On the growth of the hurricane depression. *J. Atmos. Sci.*, **21**, 68–75.

Geisler, J., 1972: On the vertical distribution of latent heat release and the mechanics of CISK. *J. Atmos. Sci.*, **29**, 240–243.

Gray, W. M., 1968: Global view of the origin of tropical disturbances and storms. *Mon. Wea. Rev.*, **96**, 669–700.

Green, J. S. A., 1965: Atmospheric tidal oscillations: An analysis of the mechanics. *Proc. Roy. Soc. London*, **A288**, 564–574.

Hayashi, Y., 1970: A theory of large-scale equatorial waves generated by condensation heat and accelerating the zonal wind. *J. Meteor. Soc. Japan*, **48**, 140–160.

——, 1971: Large-scale equatorial waves destabilized by convective heating in the presence of surface friction. *J. Meteor. Soc. Japan*, **49**, 458–465.

Holton, J. R., 1972a: *An Introduction to Dynamic Meteorology*. New York, Academic Press, 319 pp.

——, 1972b: Waves in the equatorial stratosphere generated by tropospheric heat sources. *J. Atmos. Sci.*, **29**, 368–375.

——, and D. Colton, 1972: A diagnostic study of the vorticity balance at 200 mb in the tropics during the northern summer. *J. Atmos. Sci.*, **29**, 1124–1128.

——, and R. S. Lindzen, 1968: A note on Kelvin waves in the atmosphere. *Mon. Wea. Rev.*, **95**, 385–386.

——, J. M. Wallace and J. Young, 1971: On boundary layer dynamics and the ITCZ. *J. Atmos. Sci.*, **28**, 275–280.

Joseph, D., and R. Sattinger, 1972: Stability of finite amplitude convection. *Arch. Ration. Mech. Anal.* (in press).

Kuo, H. L., 1965: On formation and intensification of tropical cyclones through latent heat release by cumulus convection. *J. Atmos. Sci.*, **22**, 40–63.

——, 1973: Planetary boundary layer flow of a stable atmosphere over the globe. *J. Atmos. Sci.*, **30**, 53–65.

Lindzen, R. S., 1966: On the relation of wave behavior to source strength and distribution in a propagating medium. *J. Atmos. Sci.*, **23**, 630–632.

——, 1967: Planetary waves on beta planes. *Mon Wea. Rev.*, **95**, 441–451.

——, 1968: Lower atmospheric energy sources for the upper atmosphere. *Meteor. Monogr.*, **9**, No. 31, 37–46.

——, 1971a: Equatorial planetary waves in shear: Part I. *J. Atmos. Sci.*, **28**, 609–622.

——, 1971b: Atmospheric tides. *Lectures in Applied Mathematics*, Vol. 14, Providence, R.I., Amer. Math. Soc., 293–362.

——, 1972: Equatorial planetary waves in shear: Part II. *J. Atmos. Sci.*, **29**, 1452–1463.

——, and T. Matsuno, 1968: On the nature of large scale wave disturbances in the equatorial lower stratosphere. *J. Meteor. Soc. Japan*, **46**, 215–221.

Longuet-Higgins, M. S., 1967: The eigenfunctions of Laplace's tidal equations over a sphere. *Phil. Trans. Soc. London*, **A262**, 511–607.

Madden, R., and P. Julian, 1972a: Further evidence of global scale, 5-day pressure waves. *J. Atmos. Sci.*, **29**, 1464–1469.

——, and ——, 1972b: Description of global-scale circulation cells in the tropics with a 40–50 day period. *J. Atmos. Sci.*, **29**, 1109–1123.

——, and E. Zipser, 1970: Multi-layered structure of the wind over the equatorial Pacific during the Line Island experiment. *J. Atmos. Sci.*, **27**, 336–342.

Martin, D. W., and V. E. Suomi, 1972: A satellite study of cloud clusters over the tropical North Atlantic Ocean. *Bull. Amer. Meteor. Soc.*, **53**, 135–156.

Morse, P. M., and H. Feshbach, 1953: *Methods of Theoretical Physics*, Part I. New York, McGraw-Hill, 997 pp.

Ooyama, K., 1971: A theory of parameterization of cumulus convection. *J. Meteor. Soc. Japan*, **49**, 744–756.

Palmén, E., and C. W. Newton, 1969: *Atmospheric Circulation Systems*. New York, Academic Press, 603 pp.

Pedlosky, J., 1970: Finite-amplitude baroclinic waves. *J. Atmos. Sci.*, **27**, 15–30.

Phillips, N. A., 1954: Energy transformations and meridional circulations associated with simple baroclinic waves in a two-level, quasi-geostrophic model. *Tellus*, **6**, 273–286.

Reed, R. J., and E. Recker, 1971: Structure and properties of synoptic-scale wave disturbances in the equatorial western Pacific. *J. Atmos. Sci.*, **28**, 1117–1133.

Riehl, H., and J. Malkus, 1958: On the heat balance in the equatorial trough zone. *Geophysica*, **6**, 503–537.

Sadler, J. C., 1969: *Average Cloudiness in the Tropics from Satellite Observations*. International Indian Ocean Expedition, Meteorological Monographs, No. 2, East-West Center Press, Honolulu.

Wallace, J. M., 1971: Spectral studies of tropospheric wave disturbances in the tropical western Pacific. *Rev. Geophys. Space Phys.*, **9**, 557–612.

Yamasaki, M., 1968: A tropical cyclone model with parameterized vertical partition of released latent heat. *J. Meteor. Soc., Japan*, **46**, 202–214.

——, 1969: Large-scale disturbances in a conditionally unstable atmosphere in low latitudes. *Pap. Meteor. Geophys.*, **20**, 289–336.

——, 1971a: Frictional convergence in Rossby waves in low latitudes. *J. Meteor. Soc. Japan*, **49**.

——, 1971b: Further study of wave disturbances in the conditionally unstable tropics. *J. Meteor. Soc. Japan*, **49**, 391–415.

Yanai, M., G. Esbensen and J. Chu, 1973: Determination of bulk properties of tropical cloud clusters from large scale heat and moisture budgets. *J. Atmos. Sci.*, **30**, 611–627.